Journal of South American Earth Sciences 140 (2024) 104898

Contents lists available at ScienceDirect

Journal of South American Earth Sciences

journal homepage: www.elsevier.com/locate/jsames

Bias-corrected high-resolution precipitation datasets assessment over a tropical mountainous region in Colombia: A case of study in Upper Cauca River Basin

Clara Marcela Romero-Hernández [a], Alvaro Avila-Diaz [a,*], Benjamin Quesada [a], Felipe Medeiros [b], Wilmar L. Cerón [c], Juan Guzman-Escalante [c], Camilo Ocampo-Marulanda [d], Roger Rodrigues Torres [e], Cristian Felipe Zuluaga [f]

[a] Earth System Science Program, Faculty of Natural Sciences, Universidad del Rosario, Bogotá D.C., Colombia
[b] Graduate Program in Climate Sciences, Federal University of Rio Grande do Norte (UFRN), Natal, Brazil
[c] Departamento de Geografía, Facultad de Humanidades, Universidad del Valle, Cali, 760032, Colombia
[d] Department of Statistics and Informatics, Federal Rural University of Pernambuco, Recife, Pernambuco, Brazil
[e] Natural Resources Institute, Universidade Federal de Itajubá, Itajubá, MG, Brazil
[f] Faculty of Agricultural Science, Corporación Universitaria Santa Rosa de Cabal - UNISARC, Santa Rosa de Cabal, Colombia

ARTICLE INFO

Keywords:
Performance metrics
Bias-correction
Climate variability
Gridded datasets

ABSTRACT

Surface gauge measurements have been commonly employed to analyze the precipitation's high spatial and temporal variability. However, incomplete area coverage and deficiencies over most tropical and complex topography mean significant limitations of this measurement type. Satellite-derived datasets, combined with the integration of in-situ observations with satellite data, are an alternative to address these limitations by offering a more spatially homogeneous and temporally comprehensive coverage for scarce data areas of the globe. Nevertheless, applying a bias correction technique on the precipitation datasets is still necessary before they are used for research due to their considerable bias. Here, we analyze the performance of CHIRPS, WorldClim, and TerraClimate datasets compared to data from 30 rain gauge stations over the South-West of Colombia, specifically in the Upper Cauca River Basin-UCRB between 1981 and 2018. Additionally, we applied the Quantile Mapping correction to all gridded precipitation products, and subsequently, the corrected rainfall is compared to the observed data on the monthly, seasonal, and annual scale. Our results show that the CHIRPS dataset better captures the seasonal and monthly variability. CHIRPS presents the best performance during less rainy seasons and at low elevation zones (900–2000 m above sea level-m.a.s.l.), followed by TerraClimate. Utilizing the bias correction methodology, we generated a new, corrected, and more reliable monthly precipitation time series for each location from all gridded precipitation products. Additionally, we found that the correction of the CHIRPS dataset presented the best performance across all spatiotemporal scales in the UCRB. Therefore, this study provides an accurate precipitation database for a complex topographic tropical region with limited data availability.

1. Introduction

Every climate system component is primarily determined by mass and energy fluxes (Jørgensen and Svirezhev, 2004). The biosphere, for example, is an open system because it exchanges energy (incoming solar radiation and outgoing longwave radiation) and mass (e.g., water, carbon dioxide, nutrients, organic matter) with the atmosphere. In this sense, precipitation is a fundamental variable of biosphere-atmosphere interaction, playing a crucial role in the water balance, water resources management, flood forecasting and serving as an input in hydrological modeling for weather and climate studies (Tapiador et al., 2017).

Typically, precipitation records have been obtained from gauge-based observation networks. However, these are subject to limitations, such as the lack of routine record-keeping, significant data gaps (Colston et al., 2018), reduced availability of long-term and high-quality

* Corresponding author.
E-mail address: alvaro.avila@urosario.edu.co (A. Avila-Diaz).

https://doi.org/10.1016/j.jsames.2024.104898
Received 27 January 2024; Received in revised form 13 April 2024; Accepted 14 April 2024
Available online 24 April 2024

information, and irregular spatial coverage. These factors restrict precipitation estimations in regions with low gauge density, such as Colombian high altitudes areas (Valencia et al., 2023). Gridded rainfall products, such as satellite, reanalysis, or multi-source merge data, provide solutions to some of these challenges since their most recent versions offer more spatially and temporally homogeneous coverage for large areas worldwide. Additionally, several high resolution climate datasets have already been constructed based on estimates from satellite and rain gauge observations (Tapiador et al., 2017). Some of them are the Climate Hazards Group InfraRed Precipitation with Stations-CHIRPS (Funk et al., 2014), which is a land-only climatic database of precipitation composed of different global sources such as satellite estimates, and in-situ observations (Katsanos et al., 2016). Both TerraClimate (Abatzoglou et al., 2018) and WorldClim (Fick and Hijmans, 2017) are a monthly climate dataset of rainfall, temperature, and other climatic variables with approximately 4 km × 4 km spatial resolution and 1 km horizontal resolution, respectively.

These datasets have been widely used in numerous studies to investigate precipitation estimates, the detection of climate variability and the evaluation of climate models at global and regional scales (Sun et al., 2018). Unfortunately, these datasets are not entirely consistent. Previous studies have shown that CHIRPS performs best in Colombia (Cepeda and Cañon, 2022; Giraldo-Osorio et al., 2022; Valencia et al., 2023). However, the product's performance depends on topographic and climatic characteristics throughout the country (Vallejo-Bernal et al., 2021). For TerraClimate and WorldClim, it is necessary to assess their performance due to the limited ground data that was used in their building and validation processes.

In that context, there is a need for evaluation and fitting the dataset outputs at different spatiotemporal scales to provide accurate information in locations with data scarcity. Several correction processes allow postprocessing procedure that corrects some statistical metrics. Bias correction corrects the mean, variance, and higher moments of climatological variables from gridded datasets (Holthuijzen et al., 2021) that come from multiple sources and have various spatial and temporal resolutions. Some advantages of the bias correction method that have made it very popular in climate data research are its relative simplicity and low computational demand (Maraun, 2016). Therefore, several bias correction methods aim to match to perfectly the mean corrected values with that of the observed ones, and they are described in detail by Teng et al. (2015) and Fang et al. (2015). Among the methods mentioned above, the Linear Scaling and the Quantile-Mapping techniques are widely used because they do not require the available time series of gauged observations to be consistent with the precipitation estimates from datasets (Tang et al., 2021). The bias correction performance depends on the location, the temporal scale, and the choice of the correction method (Chen et al., 2013) as well as the spatiotemporal settings of the data used as reference (François et al., 2020).

Precipitation exhibits significant variability over time and space, especially in mountainous regions strongly affected by macroclimate and terrain (Voropay et al., 2021). Located along the western edge of South America, the Andes Mountain Range is the world's longest continental mountain range, underscoring its significant climatic importance. Despite its importance, the rainfall network available in the Andes has significant infrastructure and maintenance limitations, resulting in low density and frequency of observations (Hobouchian et al., 2017). Although most of the existing rainfall stations in Colombia are concentrated in the Andes region, there is still a lower density coverage in the Andes and in the rest of the territory at lower altitudes (Terán-Chaves et al., 2021; Urrea et al., 2019). As a result, only a few studies have been conducted to reflect climate variability, with little work describing the climate in more specific regions in the country (Molina and Bernhofer, 2019). Several studies (Urrea et al., 2019; Villar et al., 2009) have attributed rainfall seasonality in Colombia to factors such as location, the topography, the influence of the Inter-Tropical Convergence Zone (ITCZ), the Amazon Rainforest and different phenomena in both the Pacific and Atlantic oceans.

The El Niño Southern Oscillation (ENSO) in both phases (e.g., warm (El Niño) and cold (La Niña)), emerges as one of the major phenomena significantly impacting the national territory of Colombia (Gutiérrez and Dracup, 2001). In Southwestern Colombia, during the El Niño phase, a reduced rainfall anomaly occurs, while higher rainfall conditions occur during the La Niña phase (Poveda et al., 2011). During El Niño, Colombia and the Andean region experience a dry season (with an average of 16% less total annual rainfall) and during La Niña, a wet season (with an average of 23% more total annual rainfall) (Cerón et al., 2021a).

Nevertheless, only a few studies have analyzed the accuracy of some of the high-resolution gridded datasets in representing rainfall gauge data at monthly, seasonal, and annual scales in Colombia (Cepeda and Cañon, 2022; Urrea et al., 2019), like the Cauca River Basin (CRB). This last one is Colombia's second most crucial surface water source. It is located near the Pacific Ocean and in the Andes Region, which is a region influenced by oceanic-atmospheric phenomena such as ENSO (Ávila et al., 2019) and is vulnerable to high frequency extreme events associated with hydrological hazards such as floods, landslides or severe droughts (Cerón et al., 2020a, 2020b). This significantly affects agricultural production and industrial sectors (Ávila and Carvajal, 2014), which could only worsen with the expected variability that climate change scenarios that increase variability in the CRB will bring (Poveda et al., 2011; Urrea et al., 2019).

In this sense, the relationship between different large-scale and local climate datasets varies from region to region, necessitating evaluation and correction at the regional scale (Hewitson and Crane, 2006). Furthermore, any inaccuracies in the input climate data can significantly affect modeling, calibration, and validation the models that estimate precipitation. The Upper Cauca River Basin (UCRB) is composed of the Andean range mountains, which makes it necessary to study its precipitation regime because of the high altitudes, complex terrain, difficult access due to armed conflict (Sánchez-Cuervo and Aide, 2013), large climatic gradients, and sparse and scarce data specifically for altitudes above 1000 m.a.s.l. (Condom et al., 2020). Given the CRB importance for Colombian socio-economic and ecological development and the need for the most accurate precipitation data to support decision-making for various stakeholders, we aim to obtain new best-fit datasets for the area and improved long-term gridded precipitation datasets in CRB.

For this complex topographic area, a deeper evaluation using a denser network of ground stations is needed. Our study assesses the performance of three gridded high-resolution precipitation datasets (CHIRPS, TerraClimate, and WorldClim) compared to data from 30 rain gauge stations in the UCRB in Colombia for the study period from 1981 to 2018 period, both before and after the application of bias-correction. Our scientific questions are: Which high-resolution data set can better represent rainfall in the mountainous Andean region of Colombia? How much can the precipitation datasets be improved after applying a bias correction methodology in regions with accidental topography?

2. Material and methods

2.1. Study area

From the Colombian Massif rises the Cauca River and its waters flow in a south-north direction between the Andes' Western and Central mountains. The mean longitude of the river is approximately 1,183 km until it delivers its water into the Magdalena River (Fig. 1). This basin covers an area of 66,751 km^2 with a water discharge of 76 km^3 per year (Restrepo et al., 2015). The river basin comprises four zones: Upper, Upper Valley, Middle, and Lower basin. According to the last national census in 2019 Government of Colombia's National Administrative Department of Statistics (DANE; https://www.dane.gov.co/), approximately 7 million people live in the UCRB (Upper Cauca and Upper Cauca Valley), representing 15% of the national population. The river's

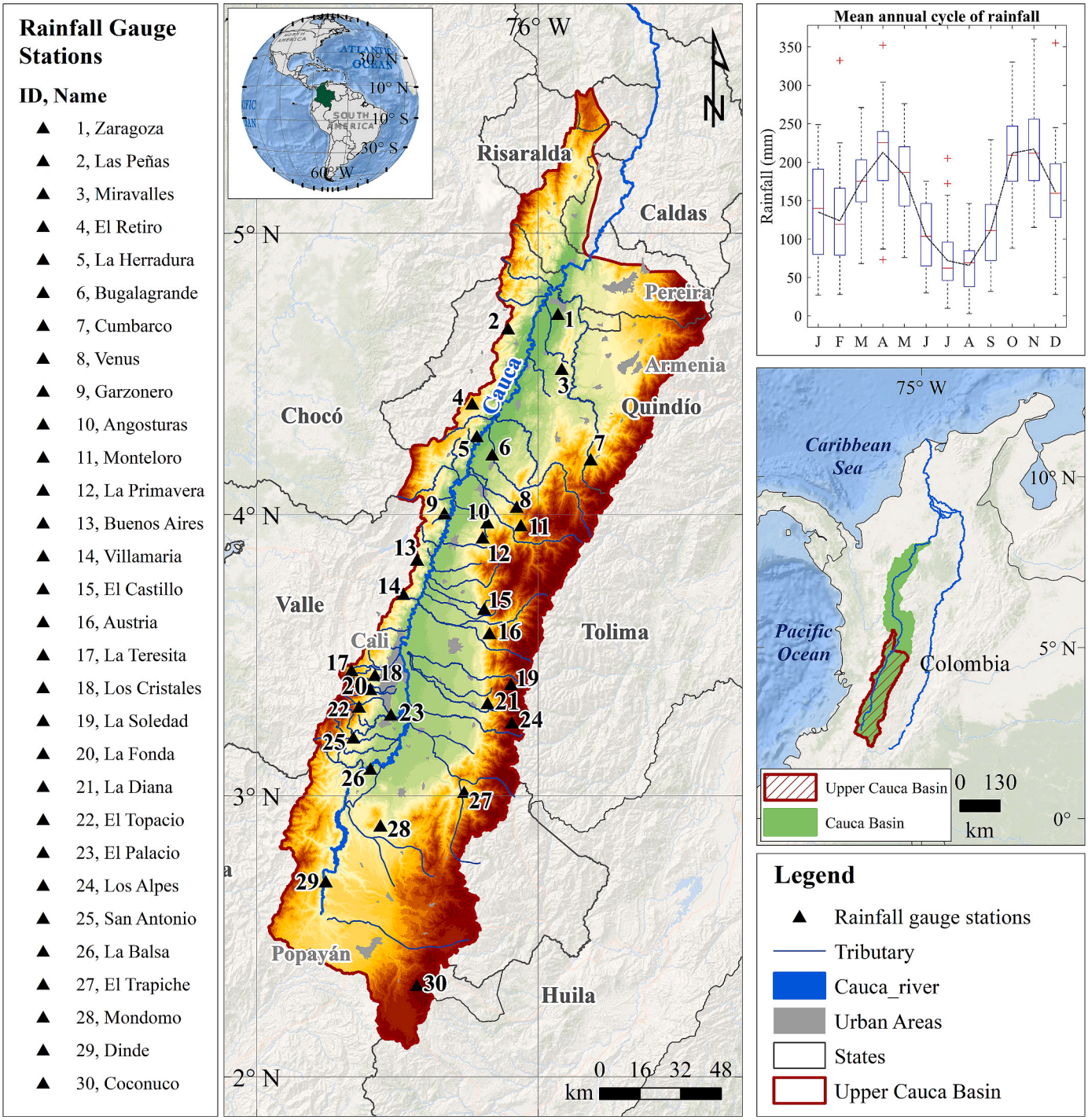

Fig. 1. Study area with gauge station's locations and monthly mean precipitation between 1981 and 2018.

elevations range from 800 to 4,900 m.a.s.l , with 39 tributaries rivers (Enciso et al., 2016).

The CRB hydro-meteorology presents a bimodal regime of rainy periods (from March to May and September to November) and less precipitation periods (December to February and June to August) (Urrea et al., 2019). The region presents a mean rainfall of 1,597 mm (±224 mm) and an air temperature of 21.3 °C (±0.5 °C) on an annual scale (Cerón et al., 2020a, 2020b). The latter is mainly influenced by a combination of meteorological systems, such as the double migration of the ITCZ and the advection of water vapor from the eastern Pacific Ocean by the Chocó jet (Sierra et al., 2021), topography and dynamics of land cover (Urrea et al., 2019). Interannual climate variability in the region is dominated by ENSO, which favors an increase in rainfall during La Niña and a decrease in precipitation during the El Niño phase (Cerón et al., 2020b, 2021b).

2.2. Site-observed and gridded product's rainfall data

Daily precipitation data was provided by the Corporación Autónoma Regional del Valle del Cauca (CVC; https://ecopedia.cvc.gov.co/portal-hidroclimatologico.html) and Instituto de Hidrología, Meteorología y Estudios Ambientales (IDEAM; https://dhime.ideam.gov.co/webgis/home/) based on historical precipitation from 39 raingauge stations.

Current precipitation datasets present a wide range of spatial

resolutions for northern South America, from 30 × 30 km to recent high-resolution data sets of 1 × 1 km (Condom et al., 2020). For this reason, it is necessary to validate and calibrate the performance of high-resolution datasets in complex topographic areas. First, the CHIRPS dataset was selected because of its lengthy trend analysis (Funk et al., 2015a) and high spatial resolution (5 × 5 km), which has a 1-day temporal resolution and can be consulted in this next link: https://www.chc.ucsb.edu/data/chirps. Funk et al. (2015a) and Urrea et al. (2019) validated the CHIRPS dataset in Colombia, demonstrating its preservation of mean and seasonality for precipitation at different time scales.

The second high resolution gridded dataset is WorldClim, available from 1960 to 2048 with a horizontal spatial resolution of 1 km. WorldClim is a global climatic-gridded dataset with popular environmental, agricultural, and ecological science usage (Fick and Hijmans, 2017). This database (https://www.WorldClim.org/data/index.html) includes monthly average climate data monitored by meteorological stations worldwide and data from the Global Historical Climate Network Dataset (GHCN).

Finally, we used the TerraClimate (Abatzoglou et al., 2018), a climatic high-resolution dataset that combines a variety of climate reanalyses at a monthly scale: WorldClim v2, CRU Ts4.0, and the Japanese JRA-55 product. TerraClimate offers high spatial resolution (4.5 km) gridded datasets and a precipitation time series from 1958 to the present. This dataset has been validated in mountainous regions in Brazilian territory (Filgueiras et al., 2022) and Colombia (Cepeda and Cañon, 2022). TerraClimate is available at https://climate.Northwestknowledge.net/TERRACLIMATE/.

2.3. Data sets quality control and selection of common period

We used one daily (CHIRPS) and two monthly (Terraclimate and Worldclim) precipitation high-resolution datasets from 1981 due to CHIRPS's restrictive temporal scale availability, the gridded high-resolution dataset with the lowest temporal coverage range from 1981 to present. Additionally, most observational datasets for the study region started in the 80s. From the 39 raingauge stations, we used data only from stations with a longer record of observations, ensuring a minimum number of stations representative of the UCRB topography.

Rain gauges with more than 5% missing data (See Table S1, supplementary material) were omitted as selection criteria as per previous studies used (Paredes-Trejo et al., 2017; Rivera et al., 2018; Zambrano-Bigiarini et al., 2017). Only data from 30 stations (Fig. 1) was selected and later transformed into monthly, seasonal, and annual scales for comparison and bias correction methods. Additionally, the spatial distribution of ground stations is highly heterogeneous, with a concentration in the Central range mountain (14 of them), followed by the Western range (10 stations), and the river Valley (6 stations). We delimited a common period between 1981 and 2018 due to the availability of the institutes datasets (e.g., the IDEAM and CVC) that record meteorological information in the region.

2.4. Statistical metrics and comparison of datasets

A point-to-pixel evaluation was carried out to represent the performance of the different global precipitation datasets more accurately in estimating spatial and temporal variability of daily precipitation. The time series of rain gauge observations were matched to the corresponding CHIRPS, TerraClimate, and WorldClim pixel over the UCRB. The performance and accuracy of precipitation datasets were evaluated for the common period from 1981 to 2018 at four temporal scales (annual, hydrological year, seasonal, and monthly scale), spatial scale (orographic analysis), and the performance of the precipitation products during the ENSO phenomenon.

The ENSO phases were defined following the Oceanic Niño Index (ONI https://origin.cpc.ncep.noaa.gov/products/analysis_monitoring/ensostuff/ONI_v5.php) provided by the U.S. National Oceanic and Atmospheric Administration (NOAA) Climate Prediction Center to classify El Niño and La Niña events in the western tropical Pacific (Table 1). The ONI is calculated as the 3-month moving average of SST anomalies in the Niño3.4 region (5° N–5° S, 170°–120° W) (Abelen et al., 2015; L'Heureux et al., 2013). The El Niño event occurs when the ONI is higher than 0.5 °C and La Niña when the ONI is lower than −0.5 °C for at least five consecutive months (Andreoli et al., 2017; Larkin and Harrison, 2005). Considering that ENSO develops in the eastern equatorial Pacific during the austral winter (June–August) and reaches its maximum in summer (December–February) (Andreoli et al., 2017, 2019; Kayano et al., 2019; Lopes et al., 2022), we analyzed the performance of raw and corrected datasets for the "Normal" (or sidereal) year from 1 January to 31 December and the hydrological year defined as 1 June to 31 May (Giraldo-Osorio et al., 2022; Poveda et al., 2005).

Four statistical performance metrics were used (Table 2): the Kling-Gupta Efficiency (KGE), the percent bias (Pbias), the root mean square error (RMSE), and the mean absolute error (MAE). A KGE value of 1 indicates perfect agreement between simulations and observations. The efficiency measure of the KGE is a combination of three elements (Table 2): correlation, bias, and variability (Kling et al., 2012). The Pbias measures the average difference between the estimated and measured values, with an optimal value of 0. Values above 0 indicate overestimation bias, and the opposite means underestimation bias. The MAE provides information on the average variance between the observed and estimated datasets, considering systematic and random errors. The RMSE measures the quadratic scoring rule between the predicted and observed values. MAE and RMSE values range from 0 to ∞, with the best value at 0.

Where the letters indicate G: gauge raingauge measurement, C: global product rainfall estimate, r: linear correlation between gauge measurements and products estimates, μ: mean, σ: standard deviation, and n: number of data.

2.5. Bias correction methodology

This study used the Empirical Quantile Mapping bias correction method for precipitation estimates from gridded dataset. Quantile Mapping (QM) is a non-parametric bias correction method that does not assume any specific precipitation distribution and can apply to all precipitation datasets. This technique is chosen because it is easy to implement and has been proven effective in correcting daily and monthly precipitation (Potter et al., 2020).

The QM bias correction algorithm was applied to correct all precipitation datasets to provide better high-resolution datasets that reproduce the precipitation over the UCRB. QM has been widely used for correcting precipitation datasets (Heo et al., 2019; Themeβl et al., 2011; Yang et al., 2016). Furthermore, the QM correction method stands out for faithfully reproducing the annual precipitation cycle and the durations of wet and dry periods (Fang et al., 2015; Rajczak et al., 2016). Chen et al. (2013) observed that distribution-based methods within the QM technique consistently outperformed mean-based methods in bias correction.

The "qmap" package of Rsoftware was used to apply the bias correction to the gridded products (Gudmundsson et al., 2012). For more information, access this link https://www.rdocumentation.org/

Table 1
ENSO phases (El Niño and La Niña) evaluated years for this study.

El Niño		La Niña	
1982–83	2004–05	1983–84	2005–06
1986–87	2006–07	1984–85	2007–08
1987–88	2009–10	1988–89	2008–09
1991–92	2014–15	1995–96	2010–11
1994–95	2015–16	1998–99	2011–12
1997–98	2018–19	1999–00	2016–17
2002–03		2000–01	2017–18

Table 2
Formulas of selected performance measures based on statistical metrics.

Statistical indices	Formula
The Kling-Gupta efficiency (KGE)	$KGE = 1 - \sqrt{(r-1)^2 + \left(\frac{\sigma C}{\sigma G} - 1\right)^2 + \left(\frac{\mu C}{\mu G} - 1\right)^2}$
Percent Bias (Pbias)	$PBias = 100 \frac{\sum (C - G)}{\sum G}$
Root Mean Square Error (RMSE)	$RMSE = \sqrt{\frac{1}{n} \sum (C - G)^2}$
Mean absolute error (MAE)	$MAE = \frac{1}{n} \sum_{k=0}^{n} (\lvert C - G \rvert)$

packages/CSTools/versions/2.0.0/topics/CST_QuantileMapping).

For precipitation, we used QM that can be expressed in terms of the empirical cumulative distribution function (ecdf) and its inverse ($ecdf^{-1}$):

$$P_{cor,m,d} = ecdf^{-1}_{obs,m}\left(ecdf_{raw,m}\left(P_{raw.m,d}\right)\right)$$

$P_{cor,\ m,\ d\ =}$ Corrected precipitation on the *d*th day of *m*th month.

$P_{raw.m,d=}$Raw precipitation on the *d*th day of *m*th month.

Themeβl et al. (2011) and Enayati et al. (2021) describe the QM and use ecdfs for precipitation in their papers. Several studies affirm that the Empirical Quantile Method-EQM is effective in correcting precipitation variables (Enayati et al., 2021; Fang et al., 2015; Themeβl et al., 2011) and is attractive as a technique due to its capability to correct the mean, standard deviation, and higher-order distributional moments (Gudmundsson et al., 2012).

2.6. Trend analysis

In order to detect trends in the precipitation datasets the Theil-Sen's slope estimator (Sen, 1968) was applied. In addition, the significance of trends is calculated at the confidence level of 95% ($\alpha = 0.05$) using the Mann–Kendall test (Kendall, 1975; Mann, 1945). These non-parametric tests have been broadly used to determine climatic and hydrological tendencies (Ávila et al., 2019; Cerón et al., 2021b, 2022).

3. Results and discussion

3.1. Performance temporal analysis

3.1.1. Annual scale

In normal year, TerraClimate has the highest mean KGE value (0.50), and CHIRPS showed the worst mean KGE (0.45) for the 38-year study period (Fig. 2; left column). TerraClimate and CHIRPS show an overestimation of precipitation according to the negative mean values of Pbias (5.83% and 4.04%, respectively) (Fig. 2b). In comparison, WorldClim overestimates by 6.09%. The mean RMSE and MAE values show that CHIRPS has the lowest errors, while WorldClim has the highest errors between the three gridded products (Fig. 2c and d). For the corrected datasets, we used just the name of the dataset plus the letter "C" (e.g., CHIRPS-C, TerraClimate-C, and WorlClim-C). After the correction, the mean KGE values increased for all datasets by at least 0.1 on average, and the Pbias values of all three datasets almost reached 0.0 (Fig. 2b). Also, the corrected datasets showed a considerable reduction in error values in more than 140 mm (RMSE and MAE; Fig. 2c and d). Furthermore, the performance in the hydrological year (Fig. 2; right column) is quite similar to the normal year. Finally, CHIRPS-C showed the best capability to represent precipitation variability at these scales, followed by TerraClimate-C and WorldClim-C.

We found that the best performance on the annual scale was from CHIRPS, followed by TerraClimate and WorldClim, with the first showing the lowest mean error metrics. Both CHIRPS and TerraClimate have been evaluated in a mountainous region in Colombia by Cepeda and Cañon (2022), who found that CHIRPS had the best accuracy and performance on an annual scale compared with TerraClimate. However, TerraClimate represented temporal and spatial patterns of rainfall at this scale.

We evaluate the performance of the three databases on the annual scale considering ENSO. Despite this, the overall performance was good, optimally representing precipitation on the annual scale, even during the most extreme ENSO events. López-Bermeo et al. (2022) evaluated the performance of CHIRPS during ENSO in Antioquia (Colombia) and found similar results, indicating that CHIRPS works well in most weather conditions.

Regarding the individual performance of precipitation products in the hydrological year (Fig. 3 and Table 3), CHIRPS overestimates (underestimates) precipitation during El Niño (La Niña) events concerning the observed data, which is similar to those found by Paredes-Trejo et al. (2017). ENSO conditions are observed to impact the magnitudes of annual precipitation (Fig. S1) and hydrological years. Peaks of high rainfall coincide with La Niña events followed in 1988–1989, 1999–2001, 2008–2009, and 2010–2011. Dry years coincide with El Niño in 1982–1983, 1991–1992, 1997–1998, and 2015–2016. The results from the present study agree with several studies about the influence of ENSO on Colombian rainfall (Cerón et al., 2021a; Hoyos et al., 2013; Ocampo-Marulanda et al., 2022). Moreover, similar results were found in other regions in tropical South America, where precipitation increases (decreases) during La Niña (El Niño) events, such as in the Amazon (Jiménez-Muñoz et al., 2016) and Northeast Brazil (Medeiros and Oliveira, 2021).

3.1.2. Seasonal scale

On the seasonal scale (Fig. 4a), the mean KGE values are higher for all products during JJA and DJF, with CHIRPS presenting the highest value of 0.5 in JJA and both TerraClimate and WorldClim presented the highest values (0.53 and 0.52, respectively) during DJF. The CHIRPS dataset presented the lowest overestimation among the products evaluated, with Pbias values ranging from 2.9% to 15.4% (Fig. 4b) forall seasons. TerraClimate and WorldClim showed similar overestimations (1%–38%). Noteworthily, during the JJA season, all products showed the highest mean overestimation values among all seasons, ranging from 15.4% to 38%. Furthermore, the error metrics (RMSE and MAE; Fig. 4c and d) are higher during MAM and SON (rainy periods) than JJA and DJF (reduced precipitation periods). The characteristic of overestimation in JJA and DJF was previously reported by Ocampo-Marulanda et al. (2022) in Southwestern Nariño; also, Cepeda and Cañon (2022) noted overestimation between June and August for the upper Chicamocha river basin according to CHIRPS and TerraClimate.

The bias correction method reduced on average 25 mm for each product in the mean error values (RMSE and MAE) for the three datasets (Fig. 4c and d). Additionally, CHIRPS-C was the most accurate corrected product at the seasonal scale, with the highest KGE mean values ranging from 0.55 to 0.66 in all evaluated seasons. Furthermore, there was a larger increment in the KGE values for the CHIRPS-C dataset range from 0.14 to 0.18 than in the other products. Both TerraClimate and WorldClim presented similar values for mean error metrics and a mean KGE around 0.38 and 0.37, respectively. CHIRPS-C underestimated DJF (−7.78%) and JJA (−13.72%). Conversely, CHIRPS-C displayed overestimation in MAM and SON (around 6%).

For the ENSO years (Fig. S4), CHIRPS and WorldClim showed the best mean across all trimesters of KGE scores (CHIRPS: 0.46, WorldClim: 0.36, TerraClima: 0.34) in the La Niña years. However, in the El Niño years the KGE values are lower than La Niña years (CHIRPS: 0.35, WorldClim: 0.35, TerraClima: 0.33). After the bias correction process, CHIRPS-C showed the best performance metrics for La Niña (KGE:0.60) and El Niño (0.49).

Our Pbias analysis revealed larger overestimation values from all products (CHIRPS: 11%, TerraClimate: 10 % and WorldClim: 12%) during El Niño compared to La Niña years (CHIRPS: 2%, TerraClimate:

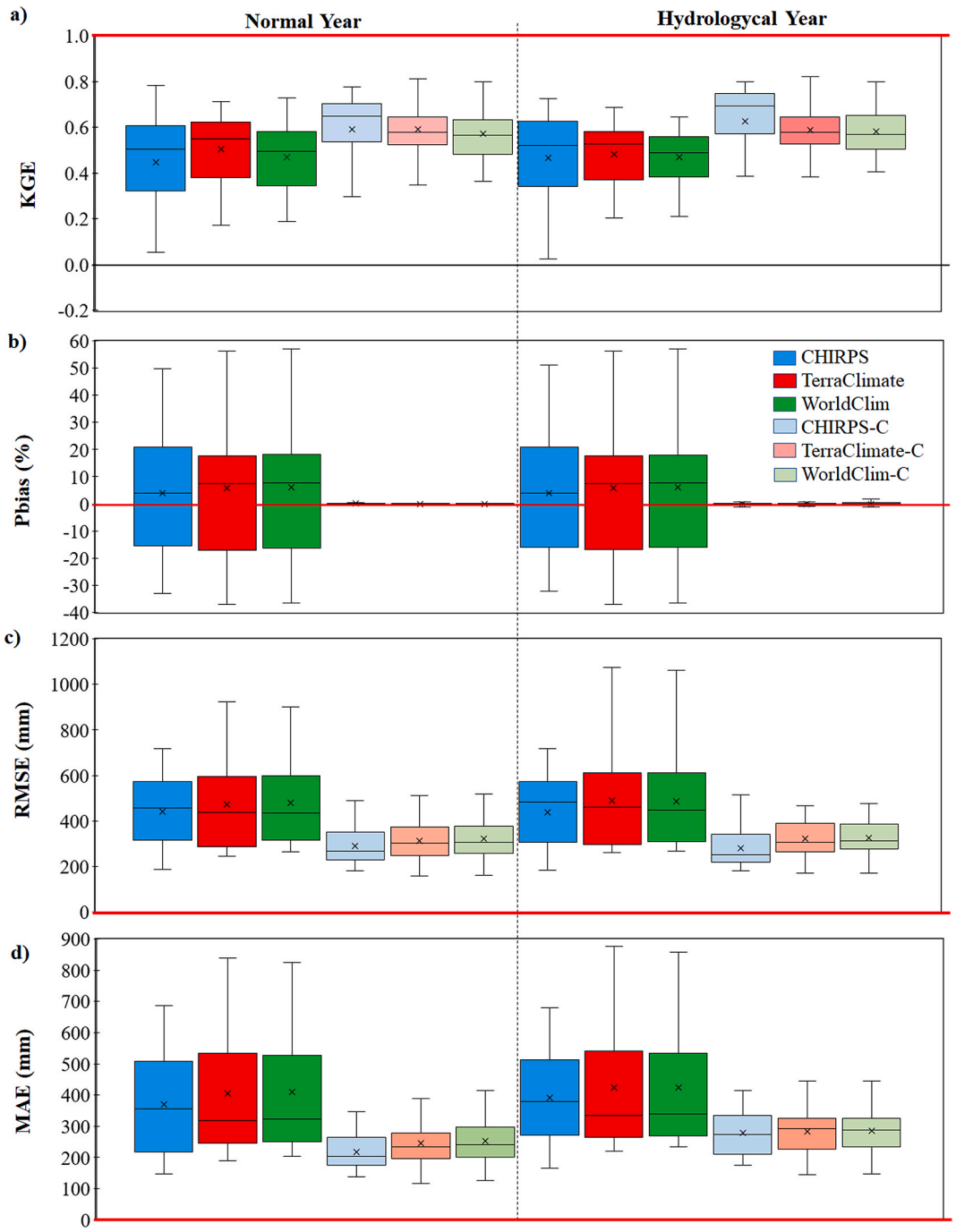

Fig. 2. Performance evaluation of precipitation datasets at an annual scale before and after the application of the bias correction: a) Kling-Gupta efficiency (KGE), b) Percent Bias (Pbias), c) Root Mean Square Error (RMSE), and d) Mean Absolute Error (MAE). The boxplots for all global products are constructed with the value of the 30 ground stations estimated over the entire period. The first (25th) and third (25th) quartiles show the interquartile spread. The red line indicates the optimum value of each metric. The letters "C" is associated with the product after the bias correction.

10%, and WorldClim: 9%). This disparity may be attributed to satellite capabilities, as they tend to have higher cloud-top temperatures, making them less effective at detecting low-level clouds (Saeidizand et al., 2018). The study area is characterized by continuous clouds cover over flat zones due to the Intertropical Convergence Zone, the Choco Low-Level Jet, orographic cloud formation mechanisms, and the dense rainforest of the Chocó region (Ocampo-Marulanda et al., 2022), further complicates satellite-based precipitation estimation by misinterpreting cloudy but dry days as rainy ones, especially in regions with lower rainfall (Saeidizand et al., 2018). Additionally, several studies have highlighted CHIRPS' limitations in discriminating between rainfall and non-rainfall events, particularly during the dry season (Paredes-Trejo et al., 2017). The reliance of CHIRPS on 0.25° TRMM (Tropical Rainfall Measuring Mission) training data may contribute to its overestimation tendency, as averaging over larger areas increases the frequency of rainfall events (Toté et al., 2015). Moreover, the sparse distribution of anchor stations could be a factor, as noted by Funk et al. (2015a). Notably, 80% of the stations used in this research do not belong to the ground station networks used by CHIRPS calibration. The reduced performance metrics observed at the yearly level compared to the monthly level, especially for CHIRPS and TerraClimate, may be ascribed to the aggregation of minor systematic biases and the presence of gaps in data

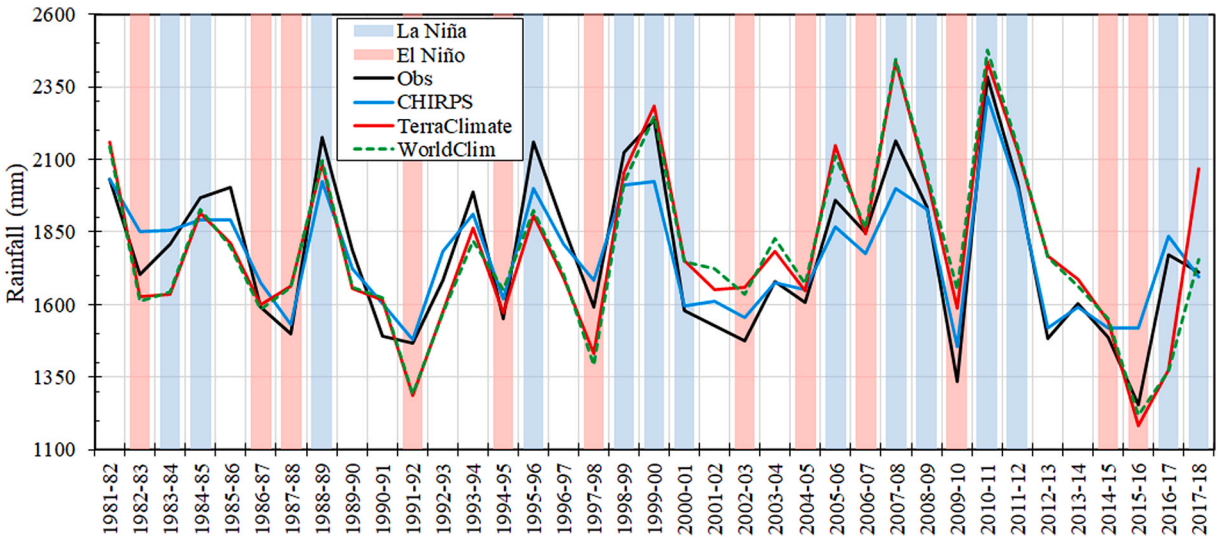

Fig. 3. Total annual precipitation in the hydrological year and from observations and CHIRPS, TerraClimate, and WorldClim datasets during the 1981–2018 period. The vertical blue and red bars in Figure b indicate La Niña and El Niño years (Table 1).

Table 3
Summary of global performance. The interannual analysis assesses the ability of global products to reproduce year-to-year (normal year/hydrological year); the seasonal analysis (DJF, MAM, JJA, and SON), and monthly variations in average before and after applying the bias correction. The values in bold indicate the best values in each performance metric.

Characteristics		CHIRPS	CHIRPS-C	TerraClimate	TerraClimate-C	WorldClim	WorldClim-C
Interannual Variability	KGE	0.45/0.46	**0.59/0.63**	0.50/0.48	**0.59/0.59**	0.47/0.47	0.57/0.58
	Pbias (%)	4.04/3.91	0.11/**-0.09**	5.83/5.71	**0.01**/−0.12	6.09/6.03	‘ −0.02/−0.11
	RMSE (mm)	440.21/437.87	**290.52/279.60**	474.57/487.90	313.48/320.72	480.02/485.99	322.89/324.72
	MAE (mm)	371.06/391.18	**216.89/227.59**	405.53/424.40	244.77/282.26	408.76/423.34	251.66/285.44
Seasonality	KGE	0.45	**0.61**	0.38	0.48	0.37	0.48
	Pbias (%)	6.18	**−2.37**	11.68	3.26	11.99	2.64
	RMSE (mm)	141.08	**116.39**	168.40	141.31	167.26	141.81
	MAE (mm)	112.51	**86.39**	135.81	108.10	135.06	108.88
Monthly	KGE	0.44	**0.60**	0.33	0.43	0.31	0.42
	Pbias (%)	6.84	−3.27	12.57	3.25	13.00	**2.52**
	RMSE (mm)	62.37	**57.41**	78.39	74.98	77.13	74.46
	MAE (mm)	48.37	**42.47**	60.74	56.73	60.24	56.69
Orographic effects and regional spatial patterns		Overall, CHIRPS, TerraClimate and WorldClim presented poor performance with high altitudes. However, CHIRPS showed the best mean statistical metrics across all evaluated elevations and temporal ranges. WorldClim and TerraClimate did show similar largest mean error values and overestimations when representing rainfall amounts at different altitudes. After the bias correction application, the new corrected datasets improved the representation of rainfall in high and medium altitudes.					

when transitioning from daily to annual time scales (Zambrano-Bigiarini et al., 2017).

Both TerraClimate and WorldClim presented the highest mean errors for both phases of ENSO, compared with the ones from CHIRPS. On the other hand, TerraClimate’s inability to capture temporal variability at finer scales than its parent datasets limit its ability to represent variability in orographic rainfall ratios and inversions. TerraClimate employs methods such as climatically aided interpolation and the combination of high-spatial-resolution climatological normals from the WorldClim dataset with coarser resolution time-varying (monthly) data to generate a monthly precipitation dataset, which inherently carries uncertainties (Fick and Hijmans, 2017).

3.1.3. Monthly scale

Before bias correction, the monthly analysis (Fig. 5) shows that CHIRPS is the most accurate product in estimating monthly precipitation amounts (KGE oscillates from −0.06 to 0.7). In addition, it provides a more accurate rainfall estimation throughout the year despite a considerable overestimation from June to August, with Pbias values ranging between 11.6% and 24.6 %). The best average KGE monthly score for CHIRPS is found in February (0.54), and the lowest is in May (0.36). TerraClimate and WorldClim are the most inaccurate products on a monthly scale, with significant rainfall underestimation from January to March (Pbias oscillates from −2.1% to −10.7%) and large overestimation from June to August (Pbias: 24.4%–58.1%). In addition, both datasets show lower KGE scores than the ones from CHIRPS for every month except for December. TerraClimate presented the lowest KGE scores in August, and WorldClim had the weakest scores in July, meaning these two products struggled to represent low-rainfall months.

The correction of the CHIRPS dataset had very good results, with an increase of at least 0.16 units in mean KGE values every month, and on average, at the monthly scale, its MAE value was reduced by 5.9 mm. So, CHIRPS-C improved mean KGE values (oscillates from 0.48 to 0.67). TerraClimate-C, on average, improves its KGE value to 0.1; the highest increments happened during low rain months such as June to August and December to January. TerraClimate and WorldClim presented reductions in mean RMSE values, with 3.4 mm for TerraClimate and 2.7 mm for WorldClim. Additionally, we evidenced a decrease in the Pbias mean values at this scale for TerraClimate (9.32 percentage points) and WorldClim (10.5 percentage points). However, CHIRPS turn from overestimating to underestimating −3.3%.

We evidenced that products struggle to accurately represent rainfall amounts during October and November due to the second rainiest season in the UCRB. This difficulty is in line with the characteristics of

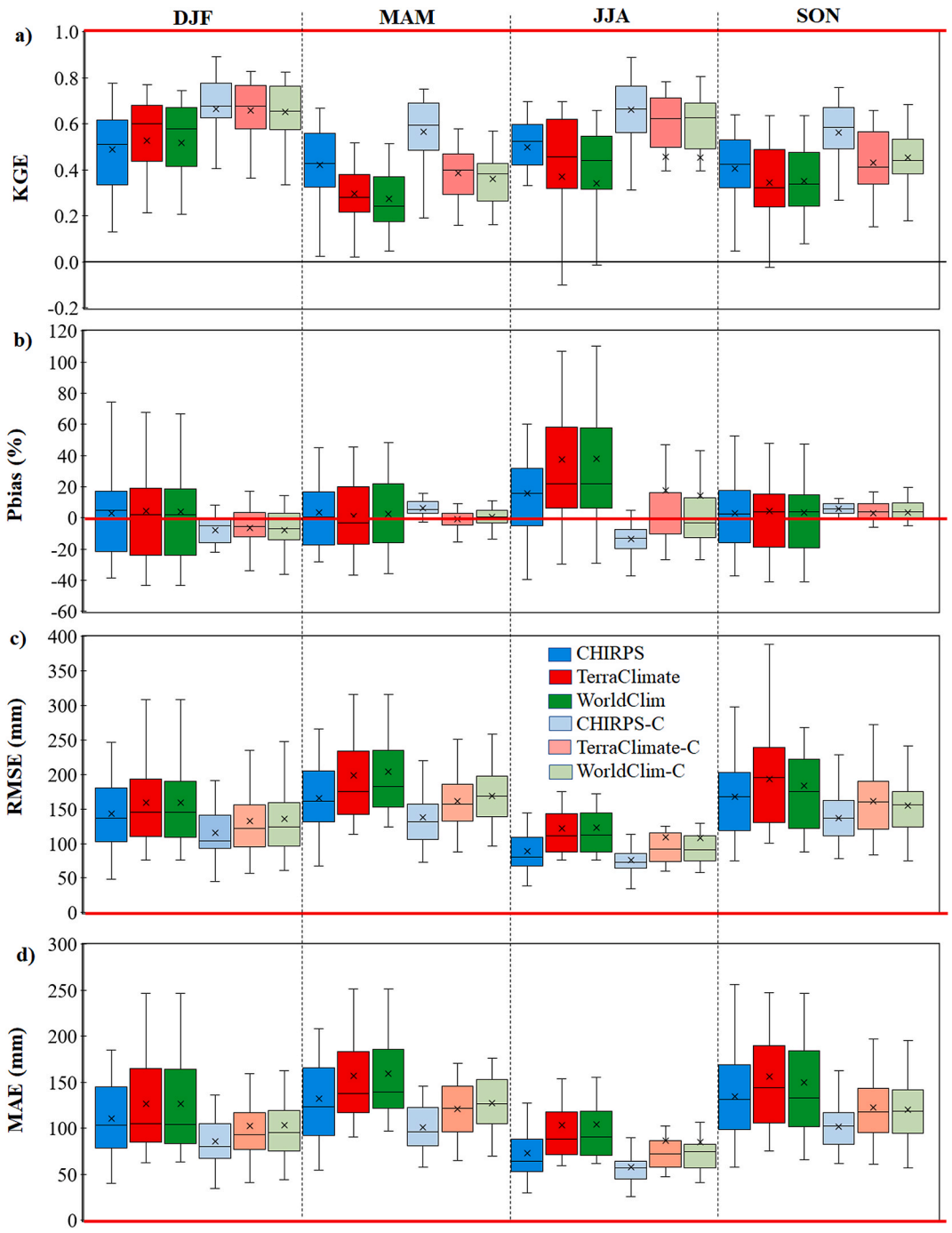

Fig. 4. Same as Fig. 2 but at seasonal scale.

satellite-based products (Qin et al., 2014), which were originally designed for lower rainfall amounts. For instance, the CHIRPS dataset tends to overestimate gauge observations but underestimates them for heavy rainfall events. The monthly performance shows concordance with the seasonal performance analysis, where it is evident that the error metrics are higher in the rainy seasons (MAM and SON). Furthermore, satellite precipitation products show evidence of estimating a higher frequency of high-intensity rain events (Sun et al., 2018). CHIRPS relies on data from the Tropical Rainfall Measuring Mission (TRMM), so any issues of overestimation or underestimation may stem from inconsistencies transferred from TRMM to CHIRPS, resulting in higher frequency estimates at high precipitation intensity bins compared to most other products (Caroletti et al., 2019).

The introduction of EQM enhanced the accuracy of all gridded rainfall datasets across various temporal scales. Specifically, the CHIRPS corrected data exhibited significantly improved proximity to the observed values at annual, seasonal, and monthly scales compared to the non-corrected condition and other corrected gridded datasets. This underscores the effectiveness of EQM in fine-tuning the dataset. TerraClimate presented an improvement in all of its statistical metrics after the EQM application, but the best results were on an annual and monthly scale. WorldClim showed a gain in all metrics after the EQM application, but the best results were on a monthly and seasonal scale. After the bias correction method, all three precipitation products showed a decrease in mean MAE and RMSE values across the four seasons.

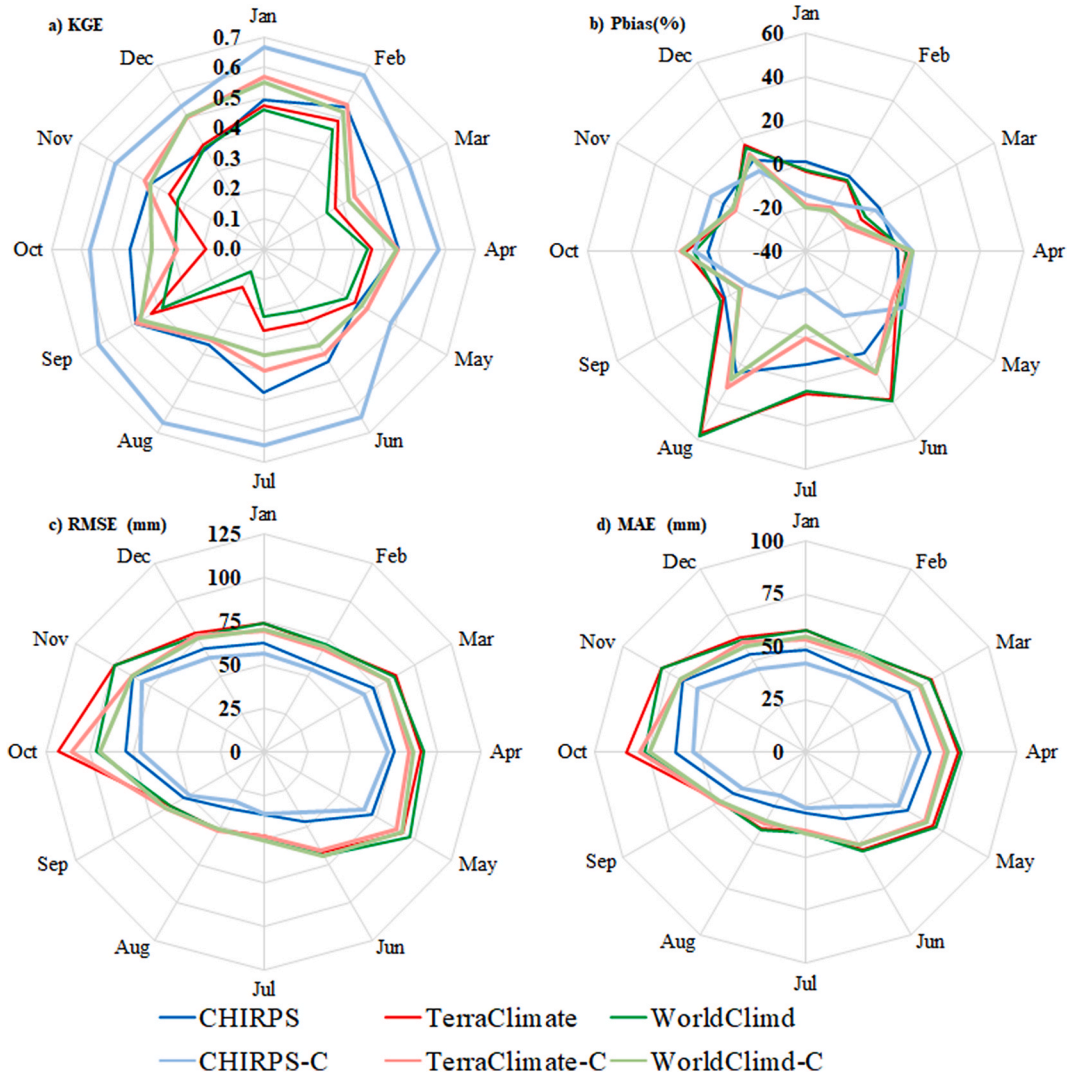

Fig. 5. Polar plot of the mean value of (a) KGE, (b) Pbias, (c) RMSE, and (d) MAE estimated for at the monthly scale. The color lines highlight the performance metrics from the three databases before and after applying the bias correction.

3.2. Orographic gradient analysis

High precipitation variability is closely tied to orographic effects, elevated altitudes, and microclimates, all impacting rainfall occurrences within the Andes Mountain Range (Riquetti et al., 2020). To quantitatively assess orographic effects, altitudinal gradients are calculated based on the altitude values specific to the mountainous systems where the stations are situated: the Central Mountain Range, the Western Mountain Range, and the valley. It is important to note that the uneven distribution of stations across regions (as outlined in Table S1 and Fig. 1 in the supplementary material) and elevation ranges (as depicted in Fig. 6) posed a challenge for a fair and unbiased comparison among different climate and elevation zones. Notably, a predominant portion of the analyzed stations, 20 out of 30, were situated within the elevation range of 1000 to 2000 m.a.s.l., while a smaller number were below 1000 m.a.s.l. (6 stations) and above 2000 m.a.s.l. (4 stations out of 30).

A drier zone emerges in the Northern region of the upper Cauca River basin due to the lower average altitude of the rainfall stations, which is consistent with the observations of Escobar et al. (2006). They described that precipitation increases proportionally to the altitude of the mountain range's slopes. Precipitation increases in function of height until it surpasses elevations above 4000 m.a.s.l.For instance, the total rainfall mean value in the Central mountain range (594.64 mm) is lower than in the western (639.19 mm) due to the higher than 4000 m.a.s.l. On the other hand, in the Valley area of the river basin (average height of 980 m.a.s.l.), the ground data shows lower precipitation values (Fig. 6). In the Central range mountain (Fig. 6), several stations are located in three altitude ranges: 1200 to 1600, 1601 to 2000, and 2001 to 3950 m.a.s.l. Several stations in the Western range mountain are in two altitude ranges: 1200 to 1600 and 1601 to 2120 m.a.s.l.

In Figs. 7 and 8, CHIRPS describes more accurately the height differences. However with higher altitudes >1400 m.a.s.l., the mean KGE metric for CHIRPS tends to decrease going from 0.52 at altitudes <1400 m.a.s.l. to 0.4 at altitudes >1700 m.a.s.l. TerraClimate and WorldClim have difficulty accurately representing precipitation values at altitudes lower than 1400 m.a.s.l and above 1700 m.a.s.l according to the large positive Pbias mean values ranging between 14.5% and 15.7%. MAM and JJA are the seasons with the most predominant low and high precipitation values in the study area, so we focused the analysis on those seasons.

During MAM (Fig. 7), we evidenced overestimation with mean Pbias values ranging between 6.4% and 14.6% according to all products, particularly CHIRPS, showing the largest mean Pbias value of 14.6% at altitudes lower than 1400 m.a.s.l., CHIRPS also showed underestimation at points lower than 1700 m.a.s.l, but higher than 1400 m.a.s.l. TerraClimate and WorldClim showed the largest mean error (MAE) values of

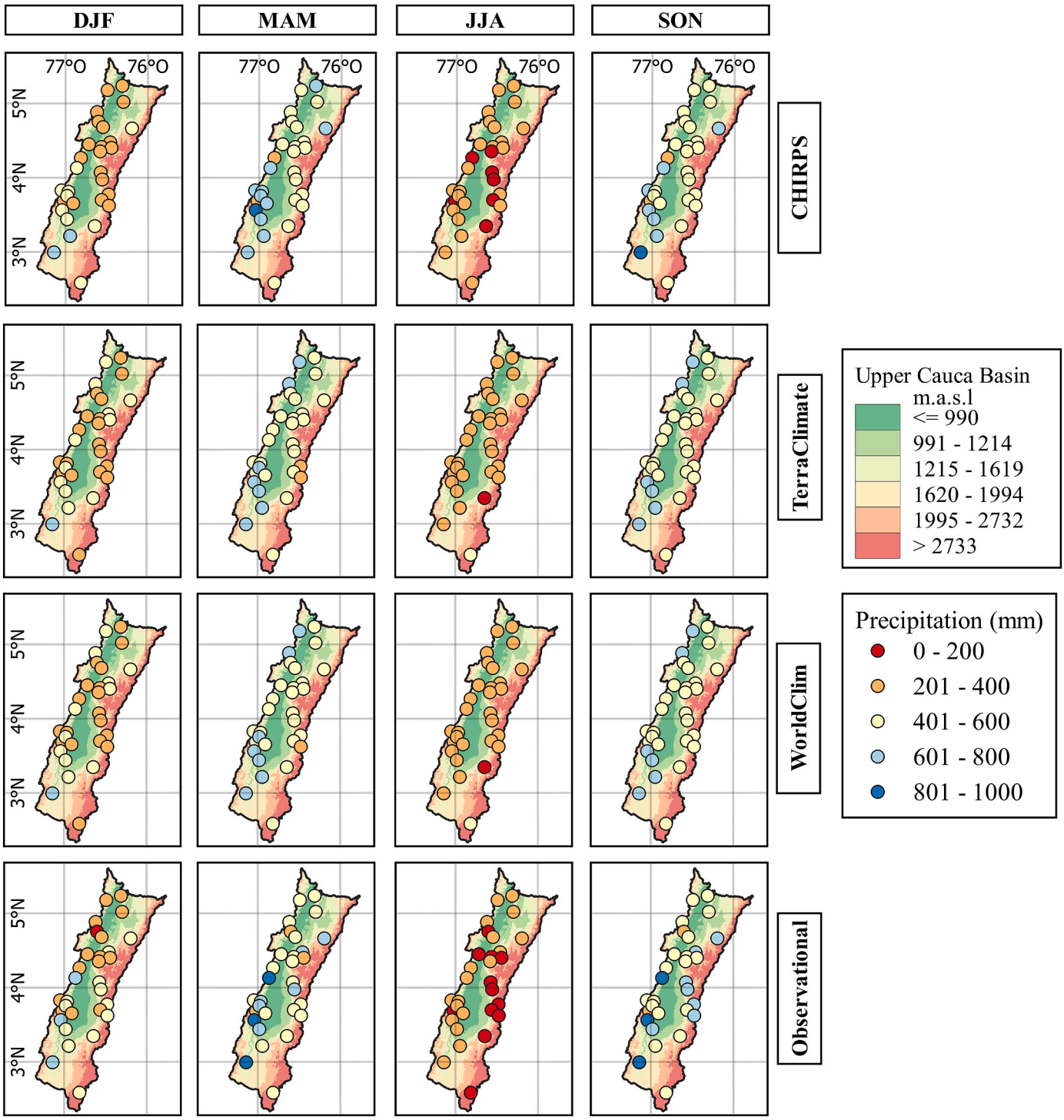

Fig. 6. Altitudinal gradient of precipitation during DJF (a), MAM (b), JJA (c) and SON (d) from raw datasets between 1981 and 2018.

181.4 mm and 183.7 mm, respectively, in altitudes between 1400 and 1700 m.a.s.l. While CHIRPS presented the highest mean MAE value (145.8 mm) in altitudes higher than 1700 m.a.s.l., at lower altitudes than 1400 m.a.s.l, CHIRPS presented the highest mean KGE value (0.5) for all products and heights. After the bias correction, some products reduced their Pbias values at altitudes lower than 1400 m.a.s.l. However, above 1700 m.a.s.l, TerraClimate and WorldClim showed the lowest reductions in their mean Pbias values.

During JJA (Fig. 8), elevations lower than 1400 ma.s.l. evidenced the highest mean KGE values ranging from 0.47 to 0.55. CHIRPS display the best mean KGE with 0.55 in altitudes <1400 m.a.s.l; in contrast, at altitudes >1700 m.a.s.l., CHIRPS exhibited the lowest mean KGE value of 0.44. At elevations higher than 1700 m.a.s.l all products show the highest mean MAE values ranging between 76.1 mm and 123.9 mm. In addition, TerraClimate and WorlClim showed the largest overestimation at heights> 1700 m.a.s.l. with 67.2% and 68.8%, respectively. After bias correction, we found that CHIRPS turn from overestimation across heights lower than 1400 m.a.s.l. and higher than 1700 m.a.s.l to underestimations across all altitudes. The mean KGE values presented increments for all products and across all elevations, with CHIRPS having the best mean KGE scores of all products, with values ranging between 0.66 and 0.67.

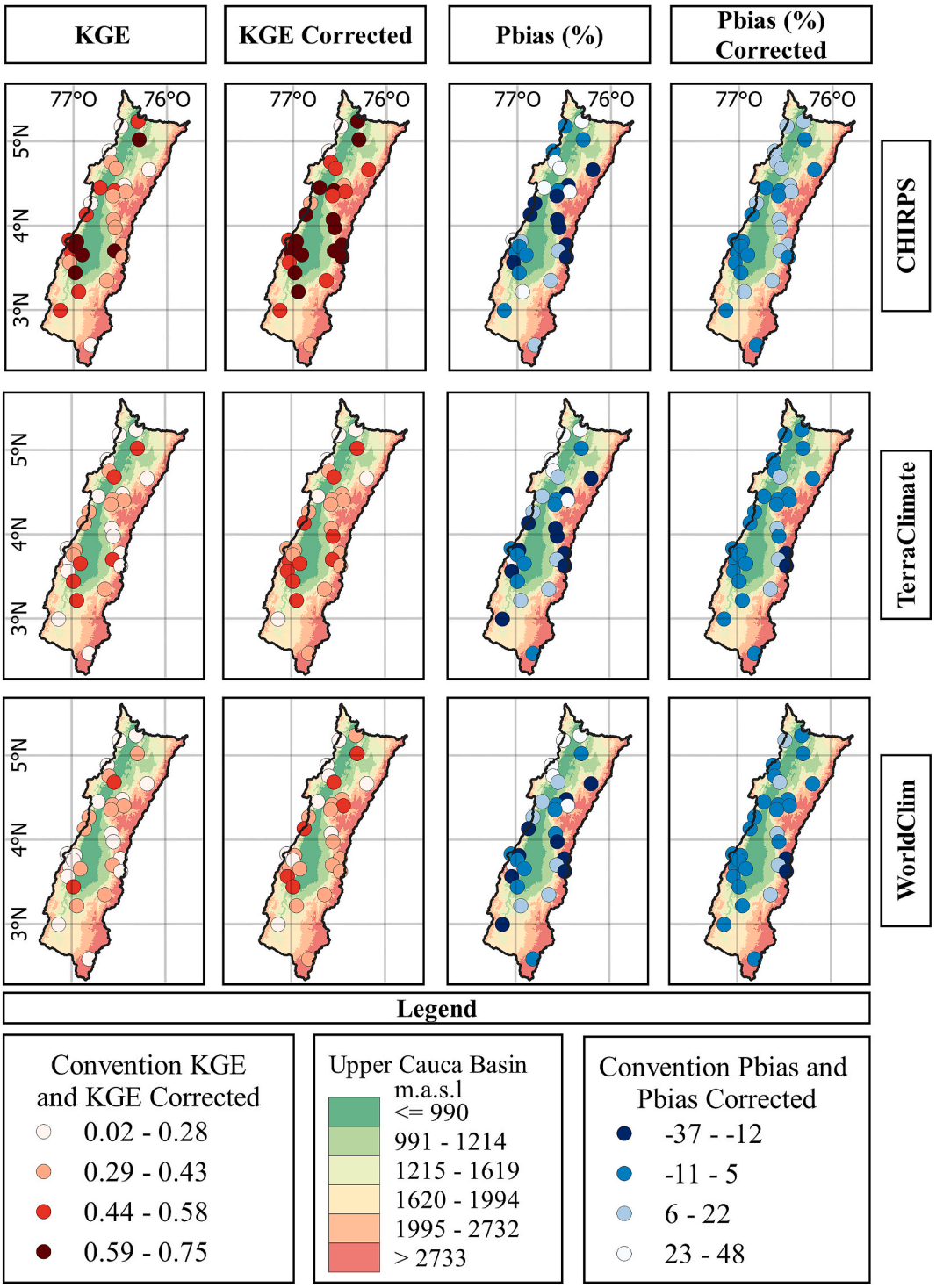

Fig. 7. Spatial distribution of KGE and Pbias (before and after bias correction) at different altitudes for the rainy season (MAM) in 1981–2018.

Lower elevations typically improve performance across the three products (Figs. 8 and 9). This is due to the observed trend that as elevation rises, the effectiveness of gridded products tends to decrease (Valencia et al., 2023). Additionally, the CHIRPS algorithms may struggle to accurately detect convective and stratiform rainfall events, according to (Arregocés et al., 2023), which makes them conclude that this limitation stems from the algorithms' failure to consider factors that influence precipitation rates below the upper cloud level. Paredes-Trejo et al. (2017) highlighted CHIRPS's tendency to underestimate monthly rainfall in orographic regions. Various studies have demonstrated the challenge gridded datasets face in accurately capturing orographic rainfall. These investigations have identified situations in which warm orographic rains, frigid surfaces, and ice-covered mountain tops tend to be erroneously identified as precipitation (Rivera et al., 2018; Toté et al., 2015; Vicente et al., 2002).

Fig. 9 illustrates that all gridded products performed poorly at higher elevations, notably between 1,700 and 3,500 m.a.s.l. Stations positioned at elevations between 1,400 and 1,700 m.a.s.l. exhibited the most favorable mean Pbias values for all products. Conversely, MAE values were higher for stations at elevations exceeding 1700 m.a.s.l. The

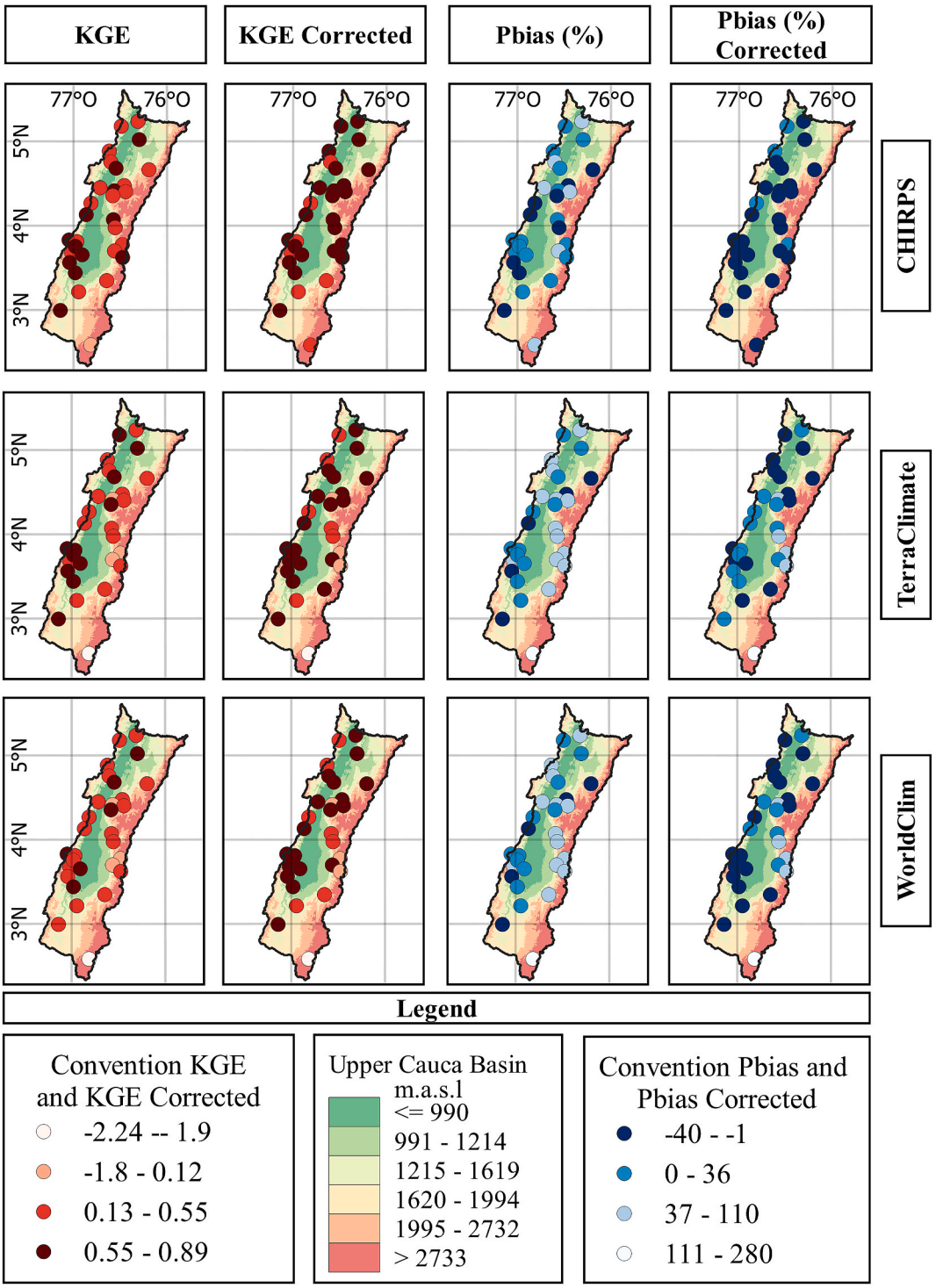

Fig. 8. Spatial distribution of KGE and Pbias (before and after bias correction) at different altitudes for the reduced rainfall season (JJA) in the 1981–2018 period.

elevation-dependent analysis suggests that the effectiveness of CHIRPS, TerraClimate, and WorldClim tends to diminish as elevation increases across all seasons (Fig. S2 and Fig. S3), as observed in previous studies (Dumont et al., 2022; Rivera et al., 2018). In different regions worldwide, TerraClimate has displayed limitations in accurately representing orographic effects (Dumont et al., 2022), while WorldClim has exhibited spatial heterogeneity influenced by local and regional topography (Wang et al., 2022).

A summary of the main results is shown in Table 3. CHIRP'sS statistical metrics show suitability at temporal and orographic scales. These findings align with the spatiotemporal assessment of gridded precipitation products made by Valencia et al. (2023). Additionally, several studies have reported that precipitation products tend to overestimate (underestimate) low (high) precipitation values in products like CHIRPS (Ocampo-Marulanda et al., 2022; Paredes-Trejo et al., 2017) for TerraClimate (Cepeda and Cañon, 2022; Dumont et al., 2022; Filgueiras et al., 2022) and WorldClim (Wang et al., 2022).

According to Toté et al. (2015), CHIRPS demonstrates limited proficiency in rainfall detection, primarily attributed to its reliance on 0.25° TRMM data. This dependence leads to an inclination for over-prediction,

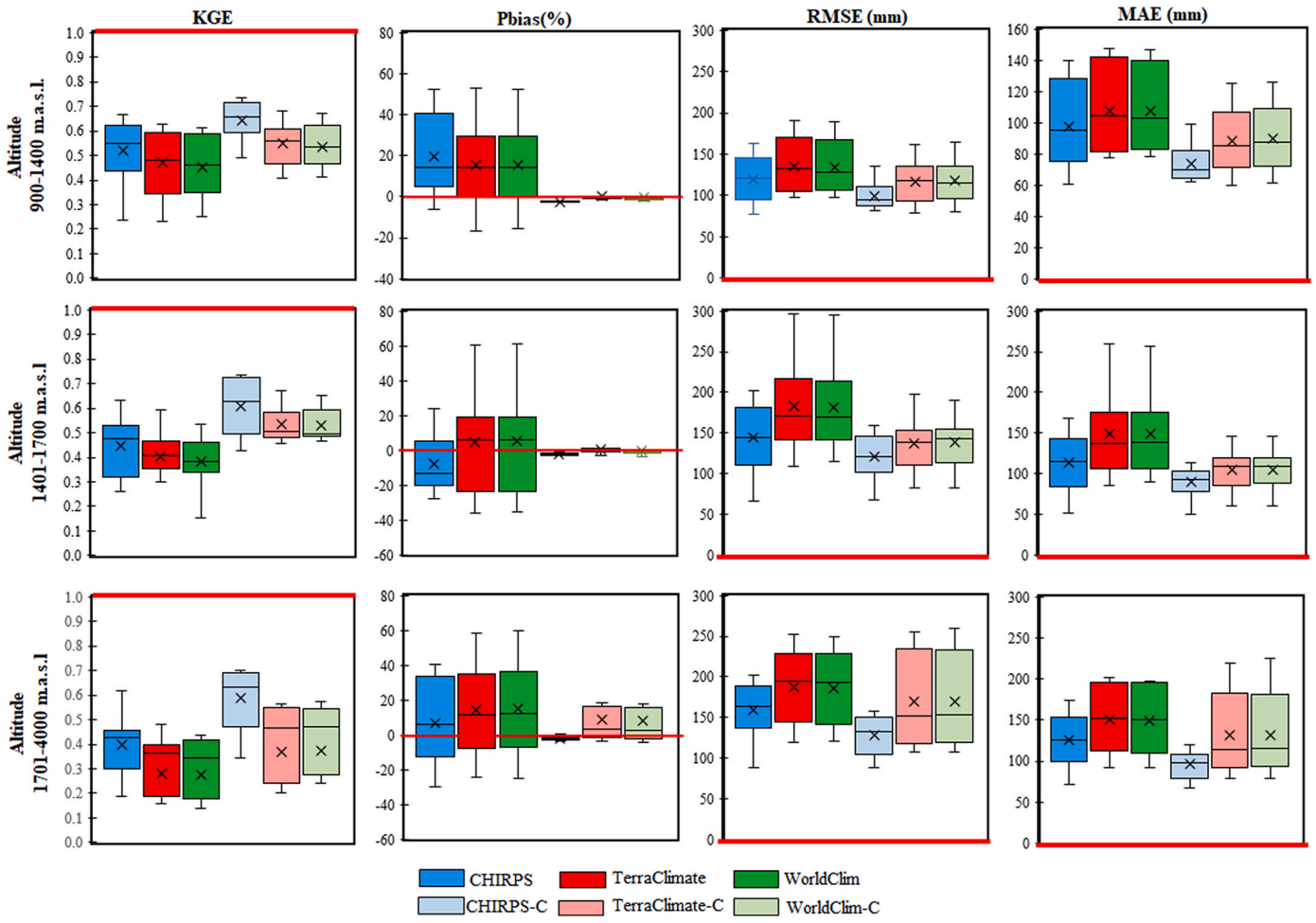

Fig. 9. Mean metrics performance of CHIRPS, TerraClimate and WorldClim using the (a) KGE, (b) RMSE, (c) Pbias and (d) MAE at a seasonal scale (DJF, MAM, JJA and SON) across the different altitudes. The red line indicates the optimum value of each metric.

as the dataset tends to do it over larger areas, amplifying the frequency of rainfall events (Toté et al., 2015). Funk et al. (2015b) suggested that this tendency may be associated with the sparse distribution of anchor stations at higher altitudes. Additionally, TerraClimate's interpolation of ground data is primarily influenced by regional rainfall patterns, resulting in a relatively modest representation of orographic effects. Consequently, TerraClimate's capability to estimate spatial rainfall patterns is constrained (Funk et al., 2015b; Toté et al., 2015).

In general, state-of-the-art precipitation datasets still retain important biases and errors in mountainous tropical areas, which can be minimized through bias correction methods, thereby improving the datasets at different spatiotemporal scales. This improvement, for example, can contribute significantly to an adequate assessment of extreme events that could result in hydrometeorological hazards in the UCRB. The outcomes indicate substantial reductions in rainfall biases at annual, seasonal, and monthly scales, significantly improving dataset accuracy. The method proves particularly effective in correcting positive biases during rainy months (Fig. S5), although certain negative biases persist, particularly in less rainy months and at higher altitudes. According to Velasquez et al. (2020), some of these remaining biases may be attributed to potential error propagation originating from interpolation methods and "gauge undercatch" in gridded observational datasets, especially in regions of high altitude where data availability is limited.

3.3. Trend analysis

Fig. 10 displays the precipitation temporal evolution from observations and datasets on annual and seasonal scales. Based on annual scale data from rainfall stations and the raw and corrected datasets, there has mostly been a decrease in precipitation levels in the study area from 1981 to 2018. Specifically, 73.3% of the observational rainfall stations reported negative trends on an annual scale and the hydrological year. In the same way, CHIRPS, CHIRPS-C, WorlClim, and WorldClim-C reproduce negative trends, but between 80 and 93% of the points evaluated. Opposite, TerraClimate, and TerraClimate-C delivered positive trends in more than 70% of the points related to the localization of stations.

Regarding trend magnitudes (Table S2 displays the average trend value over UCRB), a consistent negative trend was observed across all evaluated scales, ranging from −40.07 mm/decade to −48.23 mm/decade for the annual and hydrological year scales. CHIRPS exhibited the best performance in estimating magnitudes at these scales, with average magnitudes of −38.58 mm/decade (Annual) and −37.88 mm/decade (Hydrological year). After bias correction, CHIRPS-C improved to −48.00 mm/decade and −48.56 mm/decade, respectively. In contrast, TerraClimate and WorldClim did not closely simulate the negative trend or the magnitudes at these scales. For instance, Terraclimate showed an average of 11.09 mm/decade and WorldClim 10.55 mm/decade at the hydrological year scale.

Seasonal analysis supported these findings, a consistent negative trend across all seasons, ranging from −3.35 mm/decade to −26.3 mm/

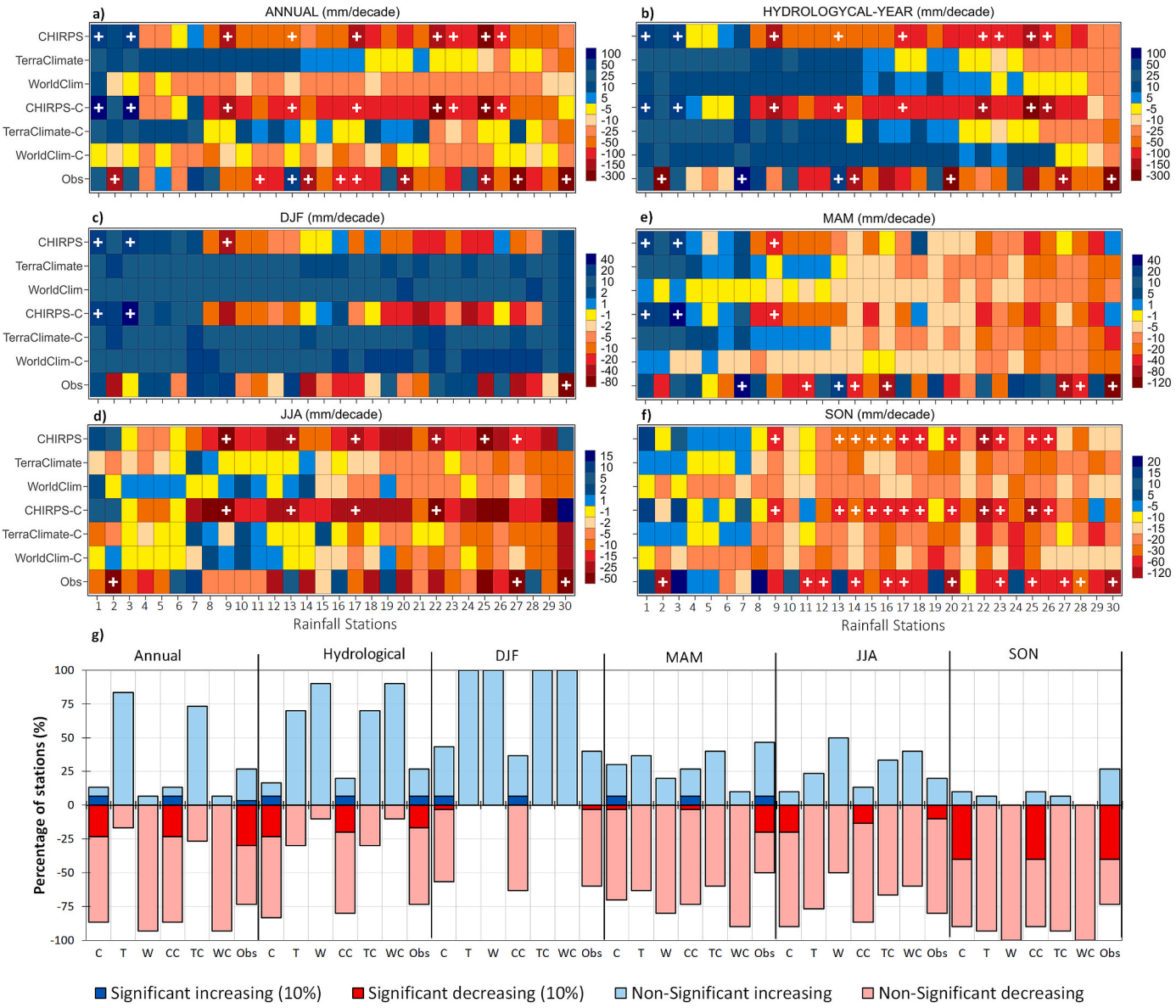

Fig. 10. (a–f) Trends per decade at annual, hydrological, and seasonal scales. (g) Percentage of stations with positive and negative trends from the total stations between 1981 and 2018. Significant trends are represented by plus symbols at the confidence level of 90% ($\alpha = 0.1$). C, T, W, CC, TC, WC and Obs indicates CHIRPS, TerraClimate, WorlClim, CHIRPS-C, TerraClimate-C, WorlClim-C, and Observation.

decade (Table S2). During the JJA, SON, and DJF, with 80%, 73.03%, and 60%, respectively, the observational stations showed a consistent decrease in precipitation. However, the signal is mixed in MAM because only 50% of stations delivered negative trends. Comparing the trend patterns with climate datasets, CHIRPS-C showed the most similar behavior to observed stations during DJF and JJA, and TerraClimate during MAM and SON. Noteworthy, in DJF, only CHIRPS and CHIRPS-C can reproduce the observation's negative trends; the rest of the raw and corrected dataset reproduces positive trends in 100% of the stations. These results align with previous studies by Ávila et al. (2019) and Puertas et al. (2008), which also found a predominance of negative trends in precipitation levels in the study area.

4. Conclusions

This study evaluated and compared three high-resolution precipitation products over UCRB between 1981 and 2018 on annual, seasonal, and monthly scales. Additionally, we investigated the performance of the best precipitation product before and after applying a bias-correction method. After bias correction, we obtained a new precipitation time series with high spatial resolution at a monthly scale, which could be an acceptable complement to sparse rain gauge observations in this Andean region characterized by complex topography and data scarcity.

The results showed that CHIRPS better captured the temporal variability of precipitation on a monthly scale compared to annually. However, CHIRPS preserved important precipitation features such as mean, total cumulative precipitation, and seasonality scales. Moreover, while CHIRPS accurately represented spatial patterns, it did not precisely depict altitudinal rainfall gradients at higher altitudes. TerraClimate exhibited suitable statistical metrics for characterizing the spatial rainfall pattern but tended to underestimate rainfall values at an annual scale in lower altitudes. WorldClim showed the highest accuracy among the three precipitation products at the interannual time scale. However, at the seasonal scale, WorldClim overestimated rainfall amounts and variability. From a spatial perspective, WorldClim showed inconsistency in representing the regional rainfall pattern and struggled to estimate rainfall in higher altitudes.

Although the three-precipitation databases represent certain aspects of rainfall over the URCB, CHIRPS emerged as the best precipitation product for the region (Table 3), a conclusion similar to those found by Cepeda and Cañon (2022) who studied the Upper Chichamocha River Basin which is located on the Eastern Cordillera of the Colombian Andes, with a mean elevation of 2874 m.a.s.l. and the altitudinal range varies between 2500 and 3950 m.a.s.l. while our study focused on the Upper Cauca River Basin, located between the Andes' Western and Central mountains and has an altitudinal range that varies between 800 and 4000 m.a.s.l.

Although the high-resolution gridded products used in this study offer valuable insights at the local scale, their usage must be conditioned by their known limits. Additionally, our findings highlight that implementing bias correction reduces the rainfall estimation error associated with regional satellite products. This underscores the crucial role of employing such methodology in hydrological studies.

The novelty of these findings lies in the fact that the monthly corrected values from high-resolution products can be used as reference values for comparing, evaluating, and calibrating global and regional climate models, which frequently lack high spatial resolution throughout the UCRB. Integrating high-quality and corrected precipitation data into hydrological or land-surface models could generate reliable outputs, particularly in applications sensitive to precipitation changes and in areas lacking meteorological stations.

CRediT authorship contribution statement

Clara Marcela Romero-Hernández: Writing – review & editing, Writing – original draft, Visualization, Validation, Supervision, Software, Methodology, Formal analysis, Data curation, Conceptualization. **Alvaro Avila-Diaz:** Writing – review & editing, Writing – original draft, Visualization, Validation, Supervision, Software, Methodology, Investigation, Formal analysis, Data curation, Conceptualization. **Benjamin Quesada:** Writing – review & editing, Writing – original draft, Visualization, Validation, Software, Methodology, Formal analysis, Data curation, Conceptualization. **Felipe Medeiros:** Writing – review & editing, Writing – original draft, Formal analysis, Data curation. **Wilmar L. Cerón:** Writing – review & editing, Writing – original draft, Visualization, Formal analysis. **Juan Guzman-Escalante:** Writing – review & editing, Writing – original draft, Visualization, Supervision, Formal analysis, Data curation. **Camilo Ocampo-Marulanda:** Writing – review & editing, Writing – original draft, Validation, Supervision. **Roger Rodrigues Torres:** Writing – review & editing, Writing – original draft, Methodology, Formal analysis. **Cristian Felipe Zuluaga:** Writing – review & editing, Writing – original draft, Supervision, Conceptualization.

Declaration of competing interest

The authors declare that they have no known competing financial interests or personal relationships that could have appeared to influence the work reported in this paper.

Data availability

The author declares that all the data used in the research are available and without access restrictions at the following link: http://www.hydroshare.org/resource/b1f1b8bd58b644229f2a77d8e886098d.

Acknowledgments

AA-D thanks the funding given by Universidad del Rosario with the project "Extremos hidroclimatológicos en Colombia durante 1980 al 2100 – EXHIDROC". W.L.C. was supported by the Universidad del Valle (Cali-Colombia) and received "Bolsista CAPES/BRASIL" grant 88887.701371/2022–00 for the development of a postdoctoral research fellowship in the Postgraduate Program in Climate and Environment (CLIAMB, INPA/UEA). BQ acknowledges support by Climat AmSud program REPRISE "Reducing climate Projection uncertainties in Southamerica" (project 21-CLIMAT-13).

Appendix A. Supplementary data

Supplementary data to this article can be found online at https://doi.org/10.1016/j.jsames.2024.104898.

References

Abatzoglou, J.T., Dobrowski, S.Z., Parks, S.A., Hegewisch, K.C., 2018. TerraClimate, a high-resolution global dataset of monthly climate and climatic water balance from 1958-2015. Sci. Data 5, 1–12. https://doi.org/10.1038/sdata.2017.191.

Abelen, S., Seitz, F., Abarca-del-Rio, R., Güntner, A., 2015. Droughts and floods in the La Plata Basin in soil moisture data and GRACE. Rem. Sens. 7, 7324–7349. https://doi.org/10.3390/rs70607324.

Andreoli, R.V., de Oliveira, S.S., Kayano, M.T., Viegas, J., de Souza, R.A.F., Candido, L. A., 2017. The influence of different El Niño types on the South American rainfall. Int. J. Climatol. 37, 1374–1390. https://doi.org/10.1002/joc.4783.

Andreoli, R.V., Kayano, M.T., Viegas, J., de Oliveira, S.S., de Souza, R.A.F., Garcia, S.R., Rego, W.H.T., de Oliveira, M.B.L., 2019. Effects of two different La Niña types on the South American rainfall. Int. J. Climatol. 39, 1415–1428. https://doi.org/10.1002/joc.5891.

Ávila, Á., Guerrero, F., Escobar, Y., Justino, F., 2019. Recent precipitation trends and floods in the Colombian Andes. Water 11, 379. https://doi.org/10.3390/w11020379.

Arregocés, H.A., Rojano, R., Pérez, J., 2023. Validation of the CHIRPS dataset in a coastal region with extensive plains and complex topography. Case Stud. Chem. Environ. Eng. 8, 100452. https://doi.org/10.1016/j.cscee.2023.100452.

Ávila, Á.J., Carvajal, Y., 2014. Agrocombustibles y soberanía alimentaria en Colombia. Cuad. Geogr. Rev. Colomb. Geogr. 24, 43–60. https://doi.org/10.15446/rcdg.v24n1.37699.

Caroletti, G.N., Coscarelli, R., Caloiero, T., 2019. Validation of satellite, reanalysis and RCM data of monthly rainfall in Calabria (Southern Italy). Rem. Sens. 11 https://doi.org/10.3390/rs11131625.

Cepeda, E., Cañon, J., 2022. Performance of high-resolution precipitation datasets CHIRPS and TerraClimate in a Colombian high Andean Basin. Geocarto Int. 1–20. https://doi.org/10.1080/10106049.2022.2129816, 0.

Cerón, Andreoli, R.V., Kayano, M.T., Ferreira de Souza, R.A., Jones, C., Carvalho, L.M.V., Cerón, W.L., Andreoli, R.V., Kayano, M.T., de Souza, R.A.F., Jones, C., Carvalho, L. M.V., 2020a. The influence of the Atlantic Multidecadal oscillation on the Choco low-level jet and precipitation in Colombia. Atmosphere 11, 174. https://doi.org/10.3390/atmos11020174.

Cerón, Carvajal-Escobar, Y., Andreoli de Souza, R.V., Kayano, M.T., González López, N., 2020b. Spatio-temporal analysis of the droughts in Cali, Colombia and their primary relationships with the El Niño-Southern Oscillation (ENSO) between 1971 and 2011. Atmósfera 33, 51–69. https://doi.org/10.20937/ATM.52639.

Cerón, Kayano, M.T., Andreoli, R.V., Canchala, T., Carvajal-Escobar, Y., Alfonso-Morales, W., 2021a. Rainfall variability in southwestern Colombia: changes in ENSO-related features. Pure Appl. Geophys. 178, 1087–1103. https://doi.org/10.1007/s00024-021-02673-7.

Cerón, Kayano, M.T., Ocampo-Marulanda, C., Canchala, T., Rivera, I.A., Avila-Diaz, A., Andreoli, R.V., de Souza, I.P., 2021b. Spatio-temporal variability of hydroclimatology in the upper Cauca River Basin in southwestern Colombia: pre- and post-Salvajina Dam perspective. Atmosphere 12, 1527. https://doi.org/10.3390/atmos12111527.

Cerón, W.L., Andreoli, R.V., Kayano, M.T., Canchala, T., Ocampo-Marulanda, C., Avila-Diaz, A., Antunes, J., 2022. Trend pattern of heavy and intense rainfall events in Colombia from 1981–2018: a trend-EOF approach. Atmosphere 13, 156. https://doi.org/10.3390/atmos13020156.

Chen, J., Brissette, F.P., Chaumont, D., Braun, M., 2013. Finding appropriate bias correction methods in downscaling precipitation for hydrologic impact studies over North America. Water Resour. Res. 49, 4187–4205. https://doi.org/10.1002/wrcr.20331.

Colston, J.M., Ahmed, T., Mahopo, C., Kang, G., Kosek, M., de Sousa Junior, F., Shrestha, P.S., Svensen, E., Turab, A., Zaitchik, B., 2018. Evaluating meteorological data from weather stations, and from satellites and global models for a multi-site epidemiological study. Environ. Res. 165, 91–109. https://doi.org/10.1016/j.envres.2018.02.027.

Condom, T., Martínez, R., Pabón, J.D., Costa, F., Pineda, L., Nieto, J.J., López, F., Villacis, M., 2020. Climatological and hydrological observations for the South American Andes: in situ stations, satellite, and reanalysis data sets. Front. Earth Sci. 8 https://doi.org/10.3389/feart.2020.00092.

Dumont, M., Saadi, M., Oudin, L., Lachassagne, P., Nugraha, B., Fadillah, A., Bonjour, J. L., Muhammad, A.Hendarmawan, Dörfliger, N., Plagnes, V., 2022. Assessing rainfall global products reliability for water resource management in a tropical volcanic mountainous catchment. J. Hydrol. Reg. Stud. 40 https://doi.org/10.1016/j.ejrh.2022.101037.

Enayati, M., Bozorg-Haddad, O., Bazrafshan, J., Hejabi, S., Chu, X., 2021. Bias correction capabilities of quantile mapping methods for rainfall and temperature variables. J. Water Clim. Chang. 12, 401–419. https://doi.org/10.2166/wcc.2020.261.

Enciso, A.A., Carvajal, Y., Sandoval, M., Carvajal Escobar, Y., Sandoval, M., 2016. Hydrological analysis of historical floods in the upper valley of Cauca river. Ing. Y Compet. 57, 46–57. https://doi.org/10.25100/iyc.v18i1.2176 (in Spanish).

Escobar, S., Aristizabal, H., González, H., Sandoval, M., Carvajal, Y., 2006. Elaboración y Actualización de Isolíneas de Precipitación, Brillo Solar, Evaporación y Temperatura Mensual en el Valle del Cauca y la Cuenca del Alto Cauca. In: VIII Congreso Colombiano de Meteorología, pp. 5–6.

Fang, G.H., Yang, J., Chen, Y.N., Zammit, C., 2015. Comparing bias correction methods in downscaling meteorological variables for a hydrologic impact study in an arid area in China. Hydrol. Earth Syst. Sci. 19, 2547–2559. https://doi.org/10.5194/hess-19-2547-2015.

Fick, S.E., Hijmans, R.J., 2017. WorldClim 2: new 1-km spatial resolution climate surfaces for global land areas. Int. J. Climatol. 37, 4302–4315. https://doi.org/10.1002/joc.5086.

Filgueiras, R., Venancio, L.P., Aleman, C.C., Cunha, F.F. da, 2022. Comparison and calibration of terraclimate climatological variables over the Brazilian territory. J. South Am. Earth Sci. 117, 103882 https://doi.org/10.1016/j.jsames.2022.103882.

François, B., Vrac, M., Cannon, A.J., Robin, Y., Allard, D., 2020. Multivariate bias corrections of climate simulations: which benefits for which losses? Earth Syst. Dyn. 11, 537–562. https://doi.org/10.5194/esd-11-537-2020.

Funk, C.C., Peterson, P.J., Landsfeld, M.F., Pedreros, D.H., Verdin, J.P., Rowland, J.D., Romero, B.E., Husak, G.J., Michaelsen, J.C., Verdin, A.P., 2014. A quasi-global precipitation time series for drought monitoring. U.S. Geol. Surv. Data Ser. 832, 4. https://doi.org/10.3133/ds832.

Funk, Peterson, P., Landsfeld, M., Pedreros, D., Verdin, J., Shukla, S., Husak, G., Rowland, J., Harrison, L., Hoell, A., Michaelsen, J., 2015a. The climate hazards infrared precipitation with stations—a new environmental record for monitoring extremes. Sci. Data 2, 150066. https://doi.org/10.1038/sdata.2015.66.

Funk, Verdin, A., Michaelsen, J., Peterson, P., Pedreros, D., 2015b. A global satellite assisted precipitation climatology. Earth Syst. Dyn. Discuss. 8, 401–425. https://doi.org/10.5194/essdd-8-401-2015.

Giraldo-Osorio, J., Trujillo-Osorio, D., Baez-Villanueva, O., 2022. Analysis of ENSO-driven variability, and long-term changes, of extreme precipitation indices in Colombia, using the satellite rainfall estimates CHIRPS. Water 14, 1733. https://doi.org/10.3390/w14111733.

Gudmundsson, L., Bremnes, J.B., Haugen, J.E., Engen-Skaugen, T., 2012. Technical Note: downscaling RCM precipitation to the station scale using statistical transformations – a comparison of methods. Hydrol. Earth Syst. Sci. 16, 3383–3390. https://doi.org/10.5194/hess-16-3383-2012.

Gutiérrez, F., Dracup, J.A., 2001. An analysis of the feasibility of long-range streamflow forecasting for Colombia using El Niño–Southern Oscillation indicators. J. Hydrol. 246, 181–196. https://doi.org/10.1016/S0022-1694(01)00373-0.

Heo, J.-H., Ahn, H., Shin, J.-Y., Kjeldsen, T.R., Jeong, C., 2019. Probability distributions for a quantile mapping technique for a bias correction of precipitation data: a case study to precipitation data under climate change. Water 11, 1475. https://doi.org/10.3390/w11071475.

Hewitson, B.C., Crane, R.G., 2006. Consensus between GCM climate change projections with empirical downscaling: precipitation downscaling over South Africa. Int. J. Climatol. 26, 1315–1337. https://doi.org/10.1002/joc.1314.

Hobouchian, M.P., Salio, P., García Skabar, Y., Vila, D., Garreaud, R., 2017. Assessment of satellite precipitation estimates over the slopes of the subtropical Andes. Atmos. Res. 190, 43–54. https://doi.org/10.1016/j.atmosres.2017.02.006.

Holthuijzen, M.F., Beckage, B., Clemins, P.J., Higdon, D., Winter, J.M., 2021. Constructing high-resolution, bias-corrected climate products: a comparison of methods. J. Appl. Meteorol. Climatol. 60, 455–475. https://doi.org/10.1175/JAMC-D-20-0252.1.

Hoyos, N., Escobar, J., Restrepo, J., Arango, A., Ortiz, J., 2013. Impact of the 2010-2011 La Niña phenomenon in Colombia, South America: the human toll of an extreme weather event. Appl. Geogr. 39, 16–25. https://doi.org/10.1016/j.apgeog.2012.11.018.

Jiménez-Muñoz, J.C., Mattar, C., Barichivich, J., Santamaría-Artigas, A., Takahashi, K., Malhi, Y., Sobrino, J.A., Schrier, G. Van Der, 2016. Record-breaking warming and extreme drought in the Amazon rainforest during the course of El Niño 2015–2016. Sci. Rep. 6, 33130 https://doi.org/10.1038/srep33130.

Jørgensen, S.E., Svirezhev, Y.M., 2004. Towards a thermodynamic theory for ecological systems. Towards a Thermodynamic Theory for Ecological Systems. Elsevier. https://doi.org/10.1016/B978-0-08-044166-5.50016-1.

Katsanos, D., Retalis, A., Michaelides, S., 2016. Validation of a high-resolution precipitation database (CHIRPS) over Cyprus for a 30-year period. Atmos. Res. 169, 459–464. https://doi.org/10.1016/j.atmosres.2015.05.015.

Kayano, M.T., Andreoli, R.V., Souza, R.A.F. de, 2019. El Niño–Southern oscillation related teleconnections over south America under distinct Atlantic multidecadal oscillation and Pacific interdecadal oscillation backgrounds: La Niña. Int. J. Climatol. 39, 1359–1372. https://doi.org/10.1002/joc.5886.

Kendall, M., 1975. Rank Correlation Methods, fourth ed. Charles Griffin, London.

Kling, H., Fuchs, M., Paulin, M., 2012. Runoff conditions in the upper Danube basin under an ensemble of climate change scenarios. J. Hydrol. 424–425, 264–277. https://doi.org/10.1016/j.jhydrol.2012.01.011.

L'Heureux, M.L., Collins, D.C., Hu, Z.Z., 2013. Linear trends in sea surface temperature of the tropical Pacific Ocean and implications for the El Niño-Southern Oscillation. Clim. Dynam. 40, 1223–1236. https://doi.org/10.1007/s00382-012-1331-2.

Larkin, N.K., Harrison, D.E., 2005. Global seasonal temperature and precipitation anomalies during El Niño autumn and winter. Geophys. Res. Lett. 32, 1–4. https://doi.org/10.1029/2005GL022860.

Lopes, A.B., Andreoli, R.V., Souza, R.A.F., Cerón, W.L., Kayano, M.T., Canchala, T., de Moraes, D.S., 2022. Multiyear La Niña effects on the precipitation in south America. Int. J. Climatol. 1–16. https://doi.org/10.1002/joc.7847.

López-Bermeo, C., Montoya, R.D., Caro-Lopera, F.J., Díaz-García, J.A., 2022. Validation of the accuracy of the CHIRPS precipitation dataset at representing climate variability in a tropical mountainous region of South America. Phys. Chem. Earth, Parts A/B/C 127,, 103184. https://doi.org/10.1016/j.pce.2022.103184.

Mann, H.B., 1945. Nonparametric tests against trend. Econometrica 13, 245–259. https://doi.org/10.2307/1907187.

Maraun, D., 2016. Bias correcting climate change simulations - a critical review. Curr. Clim. Change Rep. 2, 211–220. https://doi.org/10.1007/s40641-016-0050-x.

Medeiros, F.J., Oliveira, C.P., 2021. Dynamical aspects of the recent strong el Niño events and its climate impacts in Northeast Brazil. Pure Appl. Geophys. 178, 2315–2332. https://doi.org/10.1007/s00024-021-02758-3.

Molina, O., Bernhofer, C., 2019. Assessment of regional and historical climate records for a water budget approach in eastern Colombia. Water 12, 42. https://doi.org/10.3390/w12010042.

Ocampo-Marulanda, C., Fernández-Álvarez, C., Cerón, W.L., Canchala, T., Carvajal-Escobar, Y., Alfonso-Morales, W., 2022. A spatiotemporal assessment of the high-resolution CHIRPS rainfall dataset in southwestern Colombia using combined principal component analysis. Ain Shams Eng. J. 13, 101739 https://doi.org/10.1016/j.asej.2022.101739.

Paredes-Trejo, F.J., Barbosa, H.A., Kumar, T.V.L., 2017. Validating CHIRPS-based satellite precipitation estimates in Northeast Brazil. J. Arid Environ. 139, 26–40. https://doi.org/10.1016/j.jaridenv.2016.12.009.

Potter, N.J., Chiew, F.H.S., Charles, S.P., Fu, G., Zheng, H., Zhang, L., 2020. Bias in dynamically downscaled rainfall characteristics for hydroclimatic projections. Hydrol. Earth Syst. Sci. 24, 2963–2979. https://doi.org/10.5194/hess-24-2963-2020.

Poveda, G., Álvarez, D.M., Rueda, Ó.A., 2011. Hydro-climatic variability over the Andes of Colombia associated with ENSO: a review of climatic processes and their impact on one of the Earth's most important biodiversity hotspots. Clim. Dynam. https://doi.org/10.1007/s00382-010-0931-y.

Poveda, G., Mesa, O.J., Salazar, L.F., Arias, P.A., Moreno, H.A., Vieira, S.C., Agudelo, P. A., Toro, V.G., Alvarez, J.F., 2005. The diurnal cycle of precipitation in the tropical Andes of Colombia. Mon. Weather Rev. 133, 228–240. https://doi.org/10.1175/MWR-2853.1.

Puertas, O.O., Carvajal-Escobar, Y., Carvajal, Y., Puertas Orozco, O., Carvajal Escobar, Y., 2008. Incidencia de El Niño-Oscilación del Sur en la precipitación y la temperatura del aire en Colombia , utilizando el Climate Explorer. Rev. Científica Ing. y Desarro. 23, 104–118.

Qin, Y., Chen, Z., Shen, Y., Zhang, S., Shi, R., 2014. Evaluation of satellite rainfall estimates over the Chinese Mainland. Rem. Sens. 6, 11649–11672. https://doi.org/10.3390/rs61111649.

Rajczak, J., Kotlarski, S., Schär, C., 2016. Does quantile mapping of simulated precipitation correct for biases in transition probabilities and spell lengths? J. Clim. 29, 1605–1615. https://doi.org/10.1175/JCLI-D-15-0162.1.

Restrepo, J., Kettner, A., Syvitski, J., 2015. Recent deforestation causes rapid increase in river sediment load in the Colombian Andes. Antrhropocene 10, 13–28. https://doi.org/10.13140/RG.2.1.2516.8087.

Riquetti, N.B., Mello, C.R., Beskow, S., Viola, M.R., 2020. Rainfall erosivity in South America: current patterns and future perspectives. Sci. Total Environ. 724, 138315 https://doi.org/10.1016/j.scitotenv.2020.138315.

Rivera, J.A., Marianetti, G., Hinrichs, S., 2018. Validation of CHIRPS precipitation dataset along the central Andes of Argentina. Atmos. Res. 213, 437–449. https://doi.org/10.1016/j.atmosres.2018.06.023.

Saeidizand, R., Sabetghadam, S., Tarnavsky, E., Pierleoni, A., 2018. Evaluation of CHIRPS rainfall estimates over Iran. Q. J. R. Meteorol. Soc. 144, 282–291. https://doi.org/10.1002/qj.3342.

Sánchez-Cuervo, A.M., Aide, T.M., 2013. Consequences of the armed conflict, forced human displacement, and land abandonment on forest cover change in Colombia: a multi-scaled analysis. Ecosystems 16, 1052–1070. https://doi.org/10.1007/s10021-013-9667-y.

Sen, P.K., 1968. Estimates of the regression coefficient based on Kendall's tau. J. Am. Stat. Assoc. 63, 1379–1389. https://doi.org/10.2307/2285891.

Sierra, J.P., Arias, P.A., Durán-Quesada, A.M., Tapias, K.A., Vieira, S.C., Martínez, J.A., 2021. The Choco low-level jet: past, present and future. Clim. Dynam. 56, 2667–2692. https://doi.org/10.1007/s00382-020-05611-w.

Sun, Q., Miao, C., Duan, Q., Ashouri, H., Sorooshian, S., Hsu, K., 2018. A review of global precipitation data sets: data sources, estimation, and intercomparisons. Rev. Geophys. 56, 79–107. https://doi.org/10.1002/2017RG000574.

Tang, X., Zhang, J., Wang, G., Ruben, G.B., Bao, Z., Liu, Y., Liu, C., Jin, J., 2021. Error correction of multi-source weighted-ensemble precipitation (MSWEP) over the Lancang-Mekong River Basin. Rem. Sens. 13, 312. https://doi.org/10.3390/rs13020312.

Tapiador, F.J., Navarro, A., Levizzani, V., García-Ortega, E., Huffman, G.J., Kidd, C., Kucera, P.A., Kummerow, C.D., Masunaga, H., Petersen, W.A., Roca, R., Sánchez, J.-L., Tao, W.-K., Turk, F.J., 2017. Global precipitation measurements for validating climate models. Atmos. Res. 197, 1–20. https://doi.org/10.1016/j.atmosres.2017.06.021.

Teng, J., Potter, N.J., Chiew, F.H.S., Zhang, L., Wang, B., Vaze, J., Evans, J.P., 2015. How does bias correction of regional climate model precipitation affect modelled runoff? Hydrol. Earth Syst. Sci. 19, 711–728. https://doi.org/10.5194/hess-19-711-2015.

Terán-Chaves, C.A., Duarte-Carvajalino, J.M., Polo-Murcia, S.M., 2021. Quality control and filling of daily temperature and precipitation time series in Colombia. Meteorol. Z. 30, 489–501. https://doi.org/10.1127/metz/2021/1077.

Themeßl, M., Gobiet, A., Leuprecht, A., 2011. Empirical-statistical downscaling and error correction of daily precipitation from regional climate models. Int. J. Climatol. 31, 1530–1544. https://doi.org/10.1002/joc.2168.

Toté, C., Patricio, D., Boogaard, H., van der Wijngaart, R., Tarnavsky, E., Funk, C., 2015. Evaluation of satellite rainfall estimates for drought and flood monitoring in Mozambique. Rem. Sens. 7, 1758–1776. https://doi.org/10.3390/rs70201758.

Urrea, V., Ochoa, A., Mesa, O., 2019. Seasonality of rainfall in Colombia. Water Resour. Res. 55, 4149–4162. https://doi.org/10.1029/2018WR023316.

Valencia, S., Marín, D.E., Gómez, D., Hoyos, N., Salazar, J.F., Villegas, J.C., 2023. Spatio-temporal assessment of Gridded precipitation products across topographic and climatic gradients in Colombia. Atmos. Res. 285, 106643 https://doi.org/10.1016/j.atmosres.2023.106643.

Vallejo-Bernal, S.M., Urrea, V., Bedoya-Soto, J.M., Posada, D., Olarte, A., Cárdenas-Posso, Y., Ruiz-Murcia, F., Martínez, M.T., Petersen, W.A., Huffman, G.J., Poveda, G., 2021. Ground validation of TRMM 3B43 V7 precipitation estimates over Colombia. Part I: monthly and seasonal timescales. Int. J. Climatol. 41, 601–624. https://doi.org/10.1002/joc.6640.

Velasquez, P., Messmer, M., Raible, C.C., 2020. A new bias-correction method for precipitation over complex terrain suitable for different climate states: a case study using WRF (version 3.8.1). Geosci. Model Dev. (GMD) 13, 5007–5027. https://doi.org/10.5194/gmd-13-5007-2020.

Vicente, G.A., Davenport, J.C., Scofield, R.A., 2002. The role of orographic and parallax corrections on real time high resolution satellite rainfall rate distribution. Int. J. Rem. Sens. 23, 221–230. https://doi.org/10.1080/01431160010006935.

Villar, J.C.E., Ronchail, J., Guyot, J.L., Cochonneau, G., Naziano, F., Lavado, W., de Oliveira, E., Pombosa, R., Vauchel, P., 2009. Spatio-temporal rainfall variability in the Amazon basin countries (Brazil, Peru, Bolivia, Colombia, and Ecuador). Int. J. Climatol. 29, 1574–1594. https://doi.org/10.1002/JOC.1791.

Voropay, N., Ryazanova, A., Dyukarev, E., 2021. High-resolution bias-corrected precipitation data over South Siberia, Russia. Atmos. Res. 254, 105528 https://doi.org/10.1016/j.atmosres.2021.105528.

Wang, S., Li, H., Zhang, M., Duan, L., Zhu, X., Che, Y., 2022. Assessing gridded precipitation and air temperature products in the Ayakkum lake, central Asia. Sustain. Times 14. https://doi.org/10.3390/su141710654.

Yang, Z., Hsu, K., Sorooshian, S., Xu, X., Braithwaite, D., Verbist, K.M.J., 2016. Bias adjustment of satellite-based precipitation estimation using gauge observations: a case study in Chile. J. Geophys. Res. Atmos. 121, 3790–3806. https://doi.org/10.1002/2015JD024540.

Zambrano-Bigiarini, M., Nauditt, A., Birkel, C., Verbist, K., Ribbe, L., 2017. Temporal and spatial evaluation of satellite-based rainfall estimates across the complex topographical and climatic gradients of Chile. Hydrol. Earth Syst. Sci. 21, 1295–1320. https://doi.org/10.5194/hess-21-1295-2017.